



北京大学物理学院
School of Physics, Peking University

Many-body perturbation theory calculations of closed-shell nuclei

Furong Xu

- i) MBPT calculations for closed-shell nuclei, with $N^3\text{LO}(\text{NN})$ (and also LQCD)
- ii) HF-RPA calculations for nuclear giant resonances, with NNLO_{sat} (NN+NNN)
- iii) Gamow shell model for resonance and continuum in weakly bound nuclei, with
CD Bonn (NN)

Using Similarity Renormalization Group (SRG), Low-momentum $V_{\text{low } k}$

*Many-body perturbation theories in modern quantum chemistry and nuclear physics,
March 26-30, 2018, CEA, Saclay, France*

For nuclear structure calculations: there are two fundamental problems

1) nuclear forces; 2) many-body methods

Ab initio nuclear structure calculations

1. Starting from realistic nuclear forces

2. Renormalization (softening) to speed up convergence

3. *Ab-initio* methods to treat many-body problems

$$\hat{H}_{int} = \sum_{i < j}^A \frac{(\vec{p}_i - \vec{p}_j)^2}{2mA} + \sum_{i < j}^A V_{NN,ij} + \sum_{i < j < k}^A V_{NNN,ijk}$$

$$H_{int} = \sum_{i=1}^A \frac{p_i^2}{2m} + \sum_{i < j} V(|\vec{r}_i - \vec{r}_j|) - \frac{P^2}{2Am}$$

$$\vec{P} = \sum_{i=1}^A \vec{p}_i$$

1. Realistic nuclear forces

Yukawa nuclear force by π meson exchange ($m_\pi \approx 200m_e$)

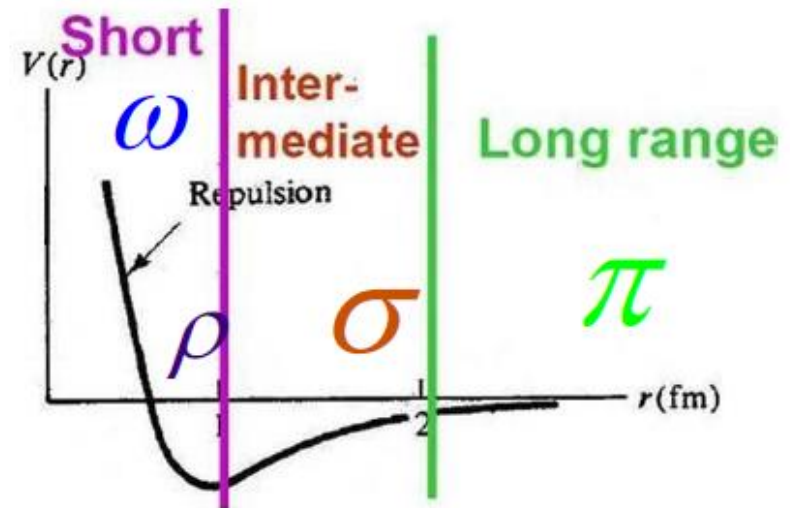
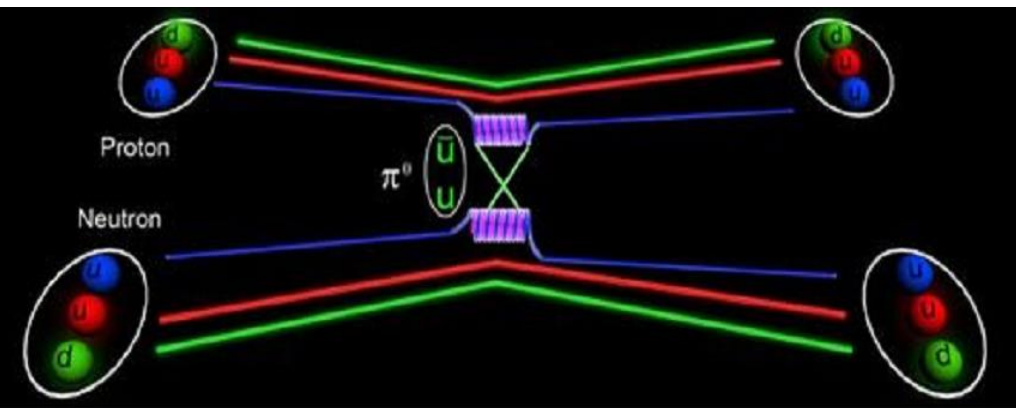
$$V(r) = -\frac{g^2}{4\pi} \frac{e^{-\frac{m_\pi c}{\hbar} r}}{r}$$

Electromagnetic force
has an infinite range!

$$V(r) \sim \frac{1}{r}$$

Long-range attractive, no short-range repulsive

Finite range:
larger mass, longer range



Nuclear force is not a fundamental interaction, but an effective force!

QCD=**quarks** + **gluons** (symmetries: spin, isospin, parity, chiral symmetry broken spontaneously)

QCD-based nuclear EFT, **Weinberg (1990's)**

Chiral EFT=**nucleons**+**pions** (symmetries: spin, isospin, parity, chiral symmetry broken spontaneously)

At low energy, the effective degrees of freedom are nucleon and pion, rather than quark and gluon!

- QCD at low energy is strong. **Perturbation is inapplicable !**
- Quarks and gluons are confined into colorless hadrons.
- Nuclear forces are residual color forces (similar to van der Waals forces)

Nuclear force



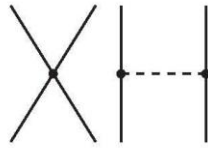
From QCD to nuclear physics via **Chiral EFT**

**Residual force of the
QCD strong interaction
outside the nucleon**

2N forces

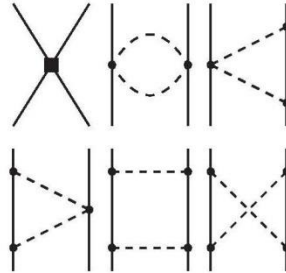
Leading
Order

Q^0
LO



Next-to
Leading
Order

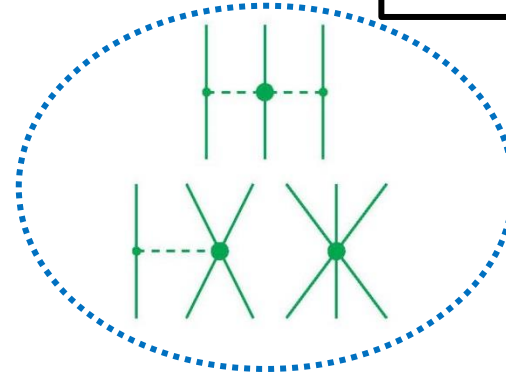
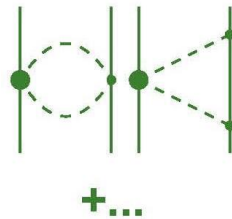
Q^2
NLO



Chiral EFT

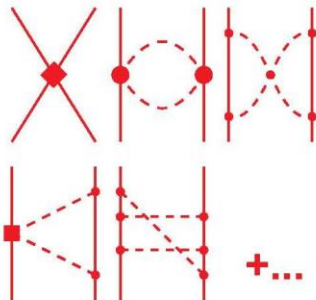
Next-to-
Next-to
Leading
Order

Q^3
 N^2LO

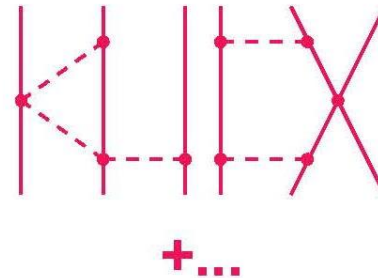


Next-to-
Next-to
Leading
Order

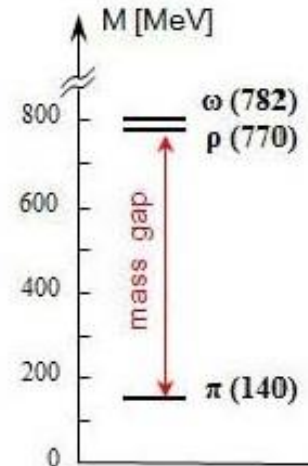
Q^4
 N^3LO



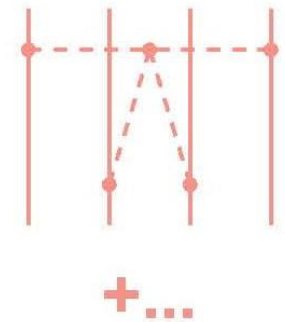
3N forces



4N forces

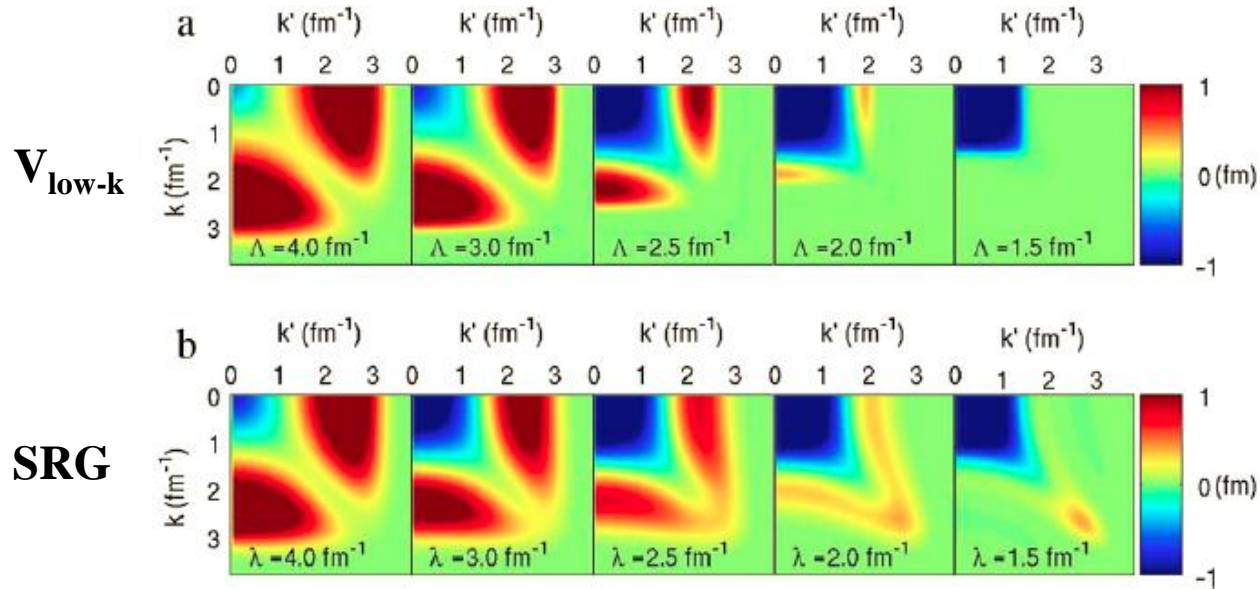
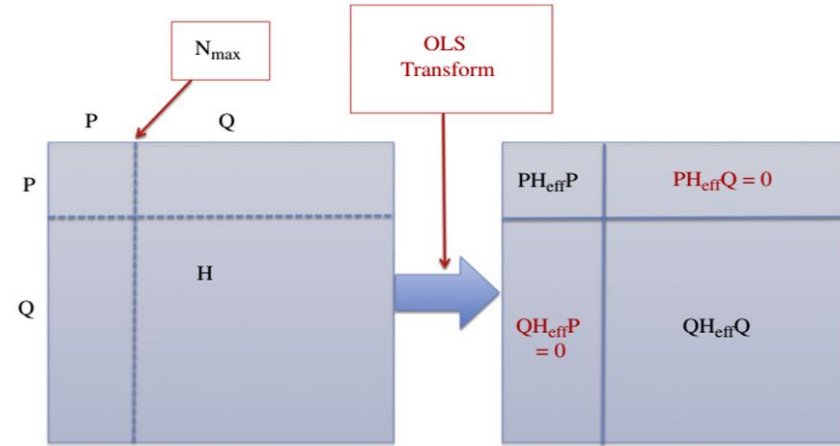
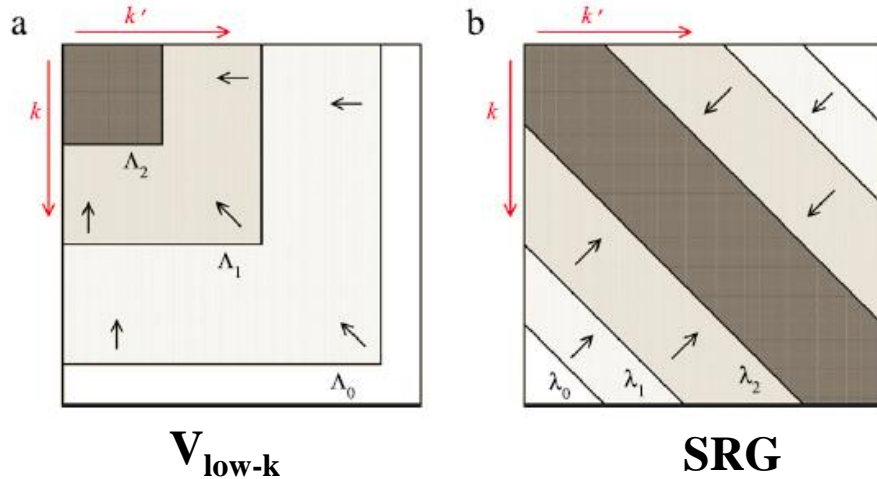


Power counting : Q/Λ



2. Renormalization

S.K. Bogner et al. / Progress in Particle and Nuclear Physics 65 (2010) 94–147



Evolutions of renormalizations for $N^3\text{LO}$

3.1 MBPT calculations for closed-shell nuclei

$$\hat{H}_{int} = \sum_{i < j}^A \frac{(\vec{p}_i - \vec{p}_j)^2}{2mA} + \sum_{i < j}^A V_{NN,ij} \quad ; \quad H_{int} = \sum_{i=1}^A \frac{p_i^2}{2m} + \sum_{i < j} V(|\vec{r}_i - \vec{r}_j|) - \frac{P^2}{2Am} \quad , \quad \vec{P} = \sum_{i=1}^A \vec{p}_i$$

- a) First we performed spherical HF calculation (in HO basis)
- b) The HF state is chosen as a reference state, which limits to closed-shell nuclei.
- c) In the HF basis, we make MBPT: for energy up to 3rd-order perturbation corrections, and for radius up to 2nd-order corrections, in the j - j scheme:

$$H_0 = \sum_{l_1 l_2} h_{l_1 l_2}^{HF} a_{l_1}^\dagger a_{l_2}$$

$$\hat{H} = \hat{H}_0 + (\hat{H} - \hat{H}_0) = \hat{H}_0 + \hat{V}$$

The exact solutions of the A-nucleon system are,

$$\hat{H}\psi_n = E_n\psi_n, \quad n = 0, 1, 2, \dots$$

The zero-order part is,

$$\hat{H}_0\phi_n = E_n^{(0)}\phi_n, \quad n = 0, 1, 2, \dots$$

For the ground state:

Perturbation (MBPT)

$$\chi_0 = \psi_0 - \phi_0$$

$$\Delta E = E_0 - E_0^{(0)}$$

$$\psi_0 = \sum_{m=0}^{\infty} [\hat{R}_0(E_0^{(0)})(\hat{V} - \Delta E)]^m \phi_0$$

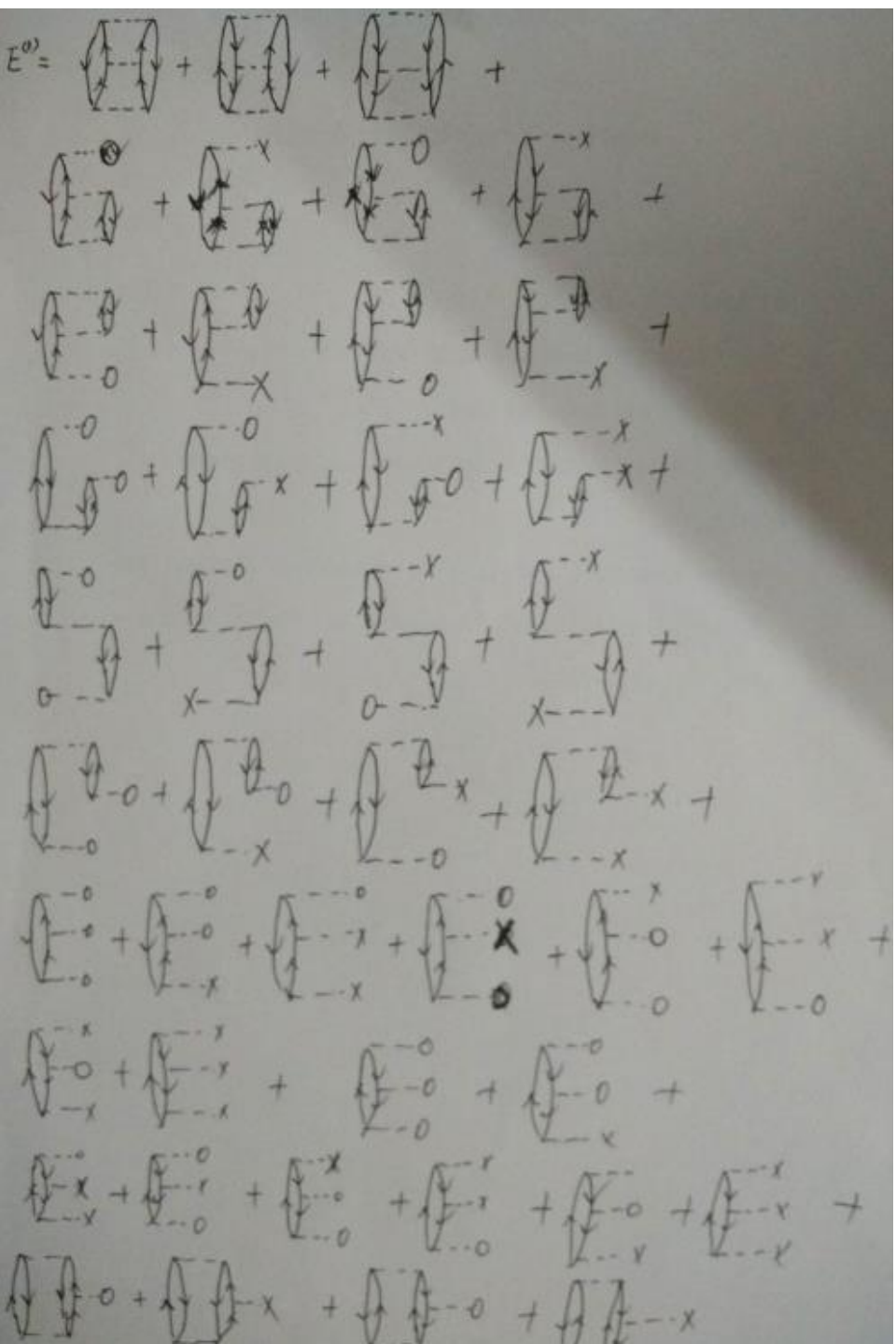
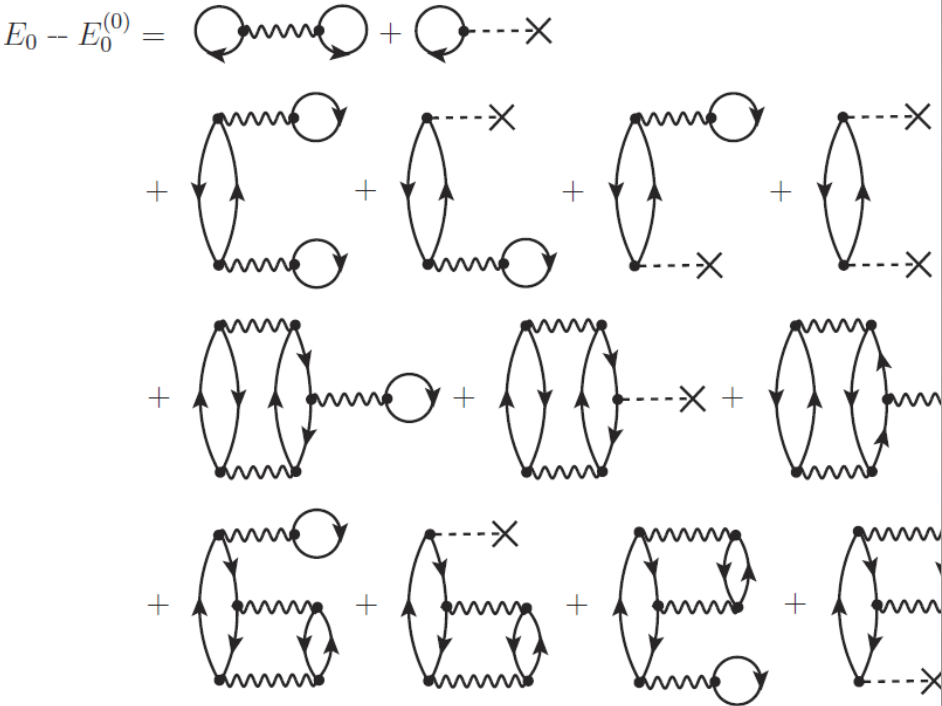
$$\Delta E = \sum_{m=0}^{\infty} \langle \phi_0 | \hat{V} [\hat{R}_0(E_0^{(0)})(\hat{V} - \Delta E)]^m | \phi_0 \rangle$$

where $\hat{R}_0 = \sum_{i \neq 0} \frac{|\phi_i\rangle\langle\phi_i|}{E_0^{(0)} - E_i^{(0)}}$ is called the resolvent of \hat{H}_0

Rayleigh-Schrodinger method

Advantages in HF basis, compared with HO b

- 1) faster convergence;
- 2) some-type perturbation diagrams are cancelled;
- 3) In HO basis, calculations could be $\hbar\omega$ dependent



$$E_0 = E_0^{(0)} + E_0^{(1)} + E_0^{(2)} + E_0^{(3)} + \dots$$

$$\text{HF energy} = \langle \phi_0 | H | \phi_0 \rangle$$

$$E_0^{(1)} = \langle \Phi_0 | \hat{V} | \Phi_0 \rangle$$

$$E_0^{(2)} = \langle \Phi_0 | \hat{V} \hat{R}_0 \hat{V} | \Phi_0 \rangle$$

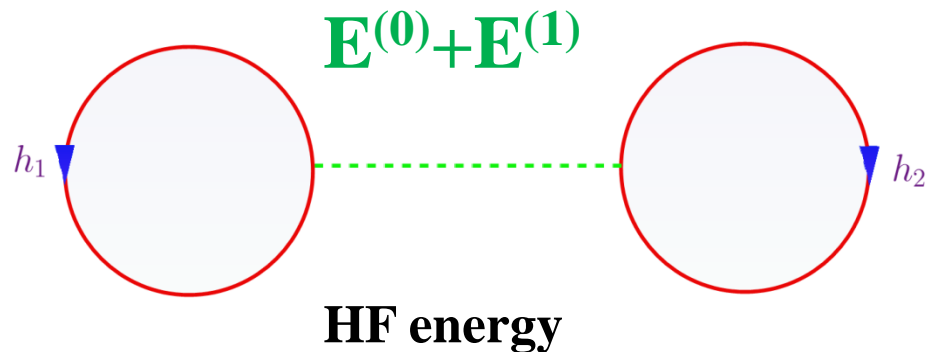
$$E_0^{(3)} = \langle \Phi_0 | \hat{V} \hat{R}_0 (\hat{V} - \langle \Phi_0 | \hat{V} | \Phi_0 \rangle) \hat{R}_0 \hat{V} | \Phi_0 \rangle$$

$$\psi_0 = \underbrace{\phi_0}_{\text{HF}} + \psi_0^{(1)} + \psi_0^{(2)} + \dots$$

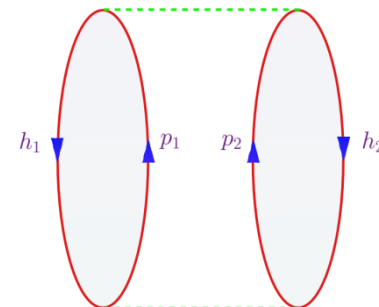
$$\psi_0^{(1)} = \hat{R}_0 \hat{V} | \Phi_0 \rangle$$

$$\psi_0^{(2)} = \hat{R}_0 (\hat{V} - E_0^{(1)}) \hat{R}_0 \hat{V} | \Phi_0 \rangle$$

Anti-Symmetrized Goldstone (ASG) diagram expansion

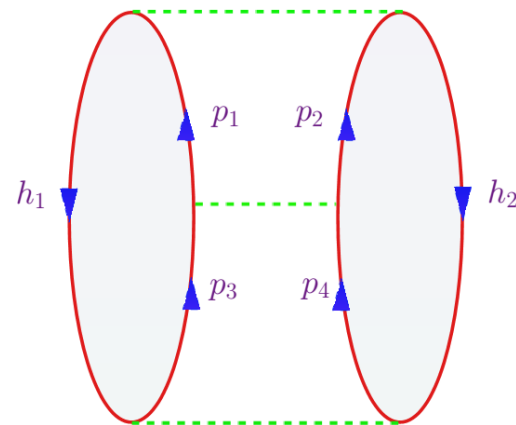
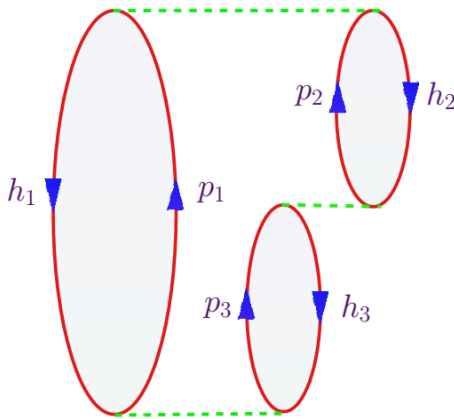
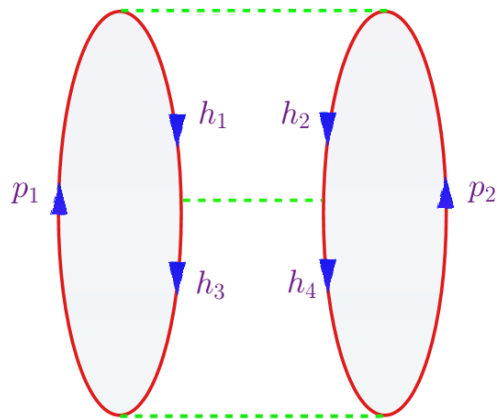


$\mathbf{E}^{(2)}$



$$\frac{1}{4} \sum_{h_1, h_2 < \varepsilon_F} \sum_{p_1, p_2 > \varepsilon_F} \frac{|\langle p_1 p_2 | \hat{H}_{int} | h_1 h_2 \rangle|^2}{\varepsilon_{h_1} + \varepsilon_{h_2} - \varepsilon_{p_1} - \varepsilon_{p_2}}$$

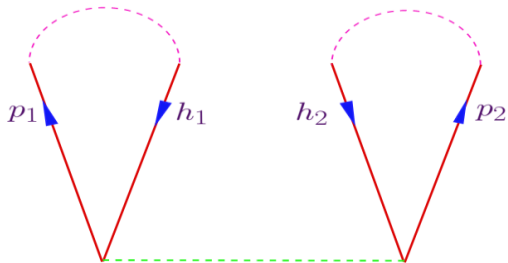
$\mathbf{E}^{(3)}$



$$2p4h = \frac{1}{8} \sum_{h_1, h_2, h_3, h_4 < \varepsilon_F} \sum_{p_1, p_2 > \varepsilon_F} \frac{\langle p_1 p_2 | \hat{H}_{int} | h_3 h_4 \rangle \langle h_3 h_4 | \hat{H}_{int} | h_1 h_2 \rangle \langle h_1 h_2 | \hat{H}_{int} | p_1 p_2 \rangle}{(\varepsilon_{h_1} + \varepsilon_{h_2} - \varepsilon_{p_1} - \varepsilon_{p_2})(\varepsilon_{h_3} + \varepsilon_{h_4} - \varepsilon_{p_1} - \varepsilon_{p_2})}$$

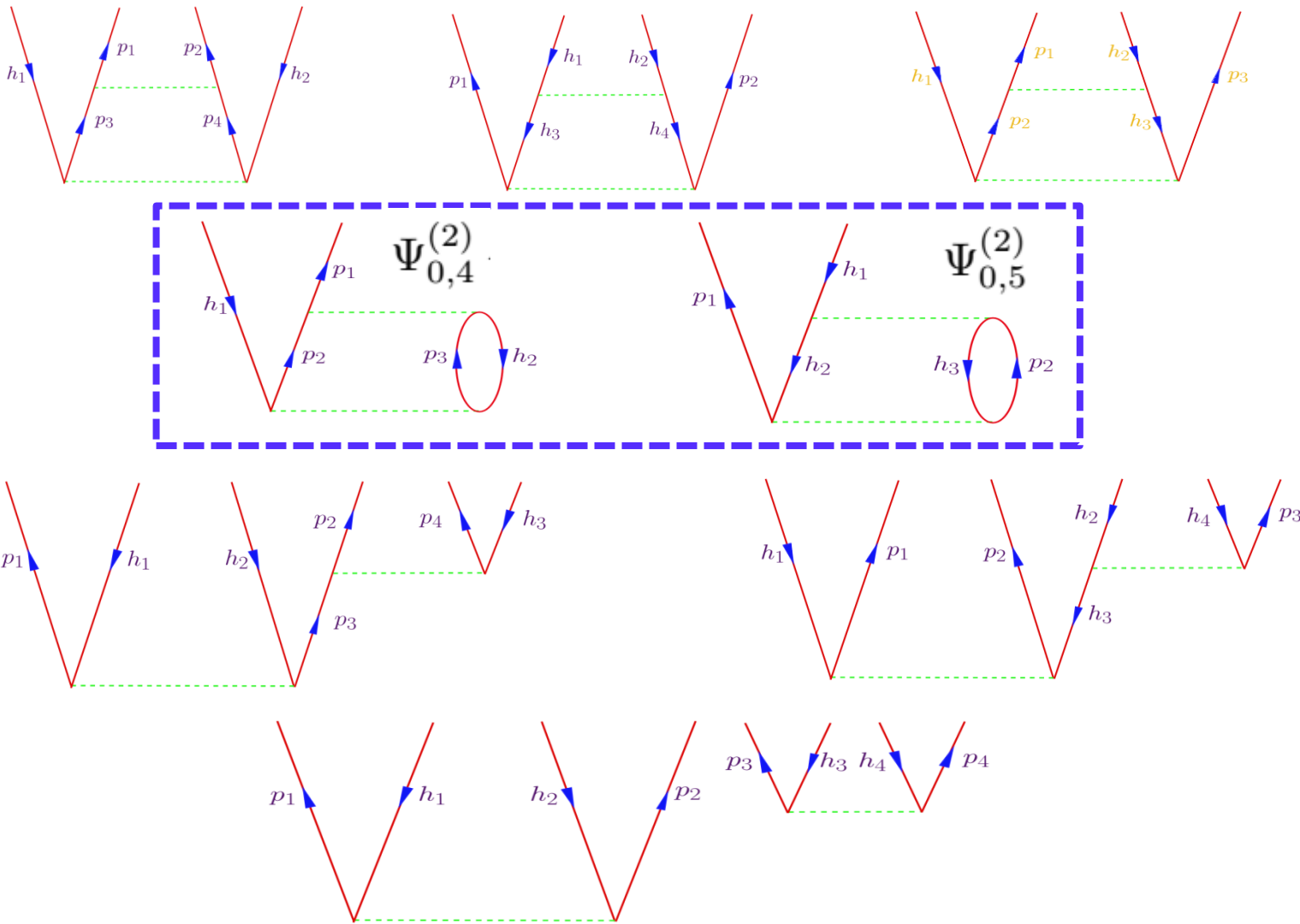
ASG diagrams for wave functions

$\psi^{(1)}$

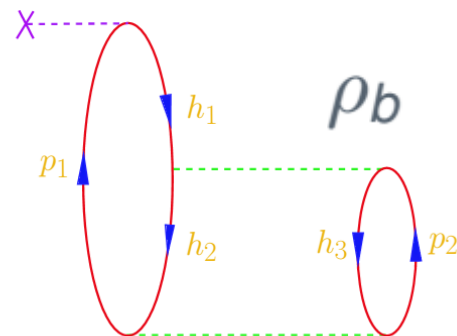
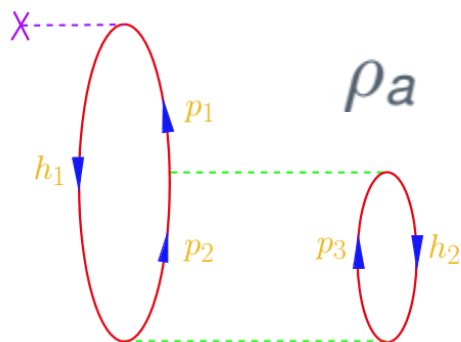


$$\Psi'_0 = \Phi_0 + \Psi_0^{(1)} + \Psi_{0,4}^{(2)} + \Psi_{0,5}^{(2)}$$

$\psi^{(2)}$

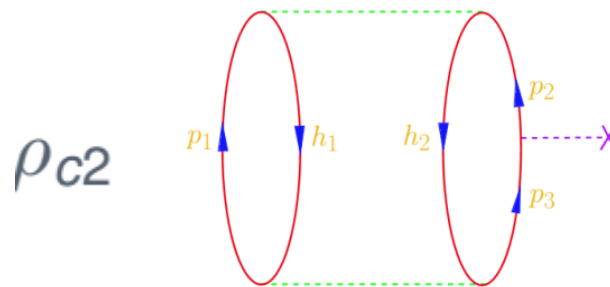
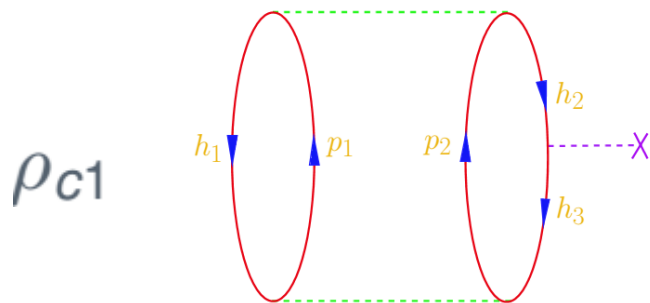


$$\rho(\vec{r}) = \underbrace{\langle \Phi_0 | \rho(\vec{r}) | \Phi_0 \rangle}_{\text{HF}} + \underbrace{\langle \Phi_0 | \rho(\vec{r}) | \Phi_0 \rangle \langle \Psi_0^{(1)} | \Psi_0^{(1)} \rangle}_{\text{2nd order}} + \underbrace{2\rho_a + 2\rho_b + \rho_{c1} + \rho_{c2} + \dots}_{\text{2nd order}}$$



$$\frac{1}{2} \sum_{h_1, h_2 < \varepsilon_F} \sum_{p_1, p_2, p_3 > \varepsilon_F} \frac{\langle h_1 h_2 | \hat{H} | p_2 p_3 \rangle \langle p_2 p_3 | \hat{H} | p_1 h_2 \rangle \langle h_1 | \rho | p_1 \rangle}{(\varepsilon_{h_1} - \varepsilon_{p_1})(\varepsilon_{h_1} + \varepsilon_{h_2} - \varepsilon_{p_2} - \varepsilon_{p_3})}$$

$$-\frac{1}{2} \sum_{h_1, h_2, h_3 < \varepsilon_F} \sum_{p_1, p_2 > \varepsilon_F} \frac{\langle p_1 p_2 | \hat{H} | h_2 h_3 \rangle \langle h_2 h_3 | \hat{H} | h_1 p_2 \rangle \langle h_1 | \rho | p_1 \rangle}{(\varepsilon_{h_1} - \varepsilon_{p_1})(\varepsilon_{h_2} + \varepsilon_{h_3} - \varepsilon_{p_1} - \varepsilon_{p_2})}$$



$$-\frac{1}{2} \sum_{h_1, h_2, h_3 < \varepsilon_F} \sum_{p_1, p_2 > \varepsilon_F} \frac{\langle h_1 h_2 | \hat{H} | p_1 p_2 \rangle \langle p_1 p_2 | \hat{H} | h_1 h_3 \rangle \langle h_3 | \rho | h_2 \rangle}{(\varepsilon_{h_1} + \varepsilon_{h_2} - \varepsilon_{p_1} - \varepsilon_{p_2})(\varepsilon_{h_1} + \varepsilon_{h_3} - \varepsilon_{p_1} - \varepsilon_{p_2})}$$

$$\frac{1}{2} \sum_{h_1, h_2 < \varepsilon_F} \sum_{p_1, p_2, p_3 > \varepsilon_F} \frac{\langle p_1 p_3 | \hat{H} | h_1 h_2 \rangle \langle h_1 h_2 | \hat{H} | p_1 p_2 \rangle \langle p_2 | \rho | p_3 \rangle}{(\varepsilon_{h_1} + \varepsilon_{h_2} - \varepsilon_{p_1} - \varepsilon_{p_3})(\varepsilon_{h_1} + \varepsilon_{h_2} - \varepsilon_{p_1} - \varepsilon_{p_2})}$$

Root-mean-square radius calculation

$$\hat{r}_m^2 = \frac{1}{A} \sum_{i=1}^A (\vec{r}_i - \vec{r}_0)^2 = \frac{1}{A^2} \sum_{i < j}^A (\vec{r}_i - \vec{r}_j)^2 = \left(1 - \frac{1}{A}\right) \left(\sum_{i=1}^A \vec{r}_i^2 / A\right) - \frac{2}{A^2} \left(\sum_{i < j}^A \vec{r}_i \cdot \vec{r}_j\right)$$

$$\approx \left(1 - \frac{1}{A}\right) \left(\sum_{i=1}^A \vec{r}_i^2 / A\right) \quad \vec{r}_0 = \frac{1}{A} \sum_{i=1}^A \vec{r}_i$$

$$\hat{r}_{pp}^2 = \frac{1}{Z} \sum_{i=1}^Z (\vec{r}_i - \vec{r}_0)^2 \approx \underbrace{\left(1 - \frac{1}{A}\right)}_{\text{c.m. effect}} \left(\sum_{i=1}^Z \vec{r}_i^2 / Z\right) \longrightarrow \langle R_{pp}^2 \rangle = \frac{\int r^2 \rho_p(\vec{r}) d^3r}{\int \rho_p(\vec{r}) d^3r}$$

$$\langle r_{ch}^2 \rangle = \langle r_{pp}^2 \rangle + R_p^2 + \frac{N}{Z} R_n^2 + \frac{3\hbar^2}{4m_p^2 c^2}$$

A. Ekstron, *et al.*, PRC 91, 051301(R) (2015).

$$R_p = 0.8775(51) \text{ fm} \quad \frac{3\hbar^2}{4m_p^2 c^2} \approx 0.033 \text{ fm}^2, \quad R_n^2 = -0.1149(27) \text{ fm}^2$$

$$\Delta r_{\text{c.m.}} = \left[\left(1 - \frac{1}{A}\right) \langle R_{pp}^2 \rangle \right]^{1/2} - \langle R_{pp}^2 \rangle^{1/2}$$

Approximate center-of-mass correction
for charge radius (point-proton)

NCSM

S.K. Bogner *et al.*,
arXiv0708.3754v2 (2007)

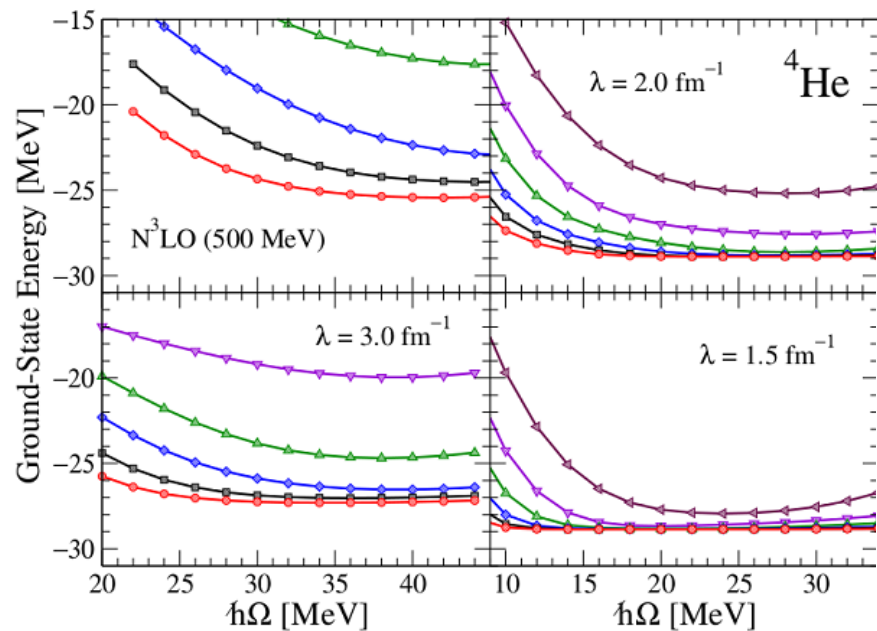


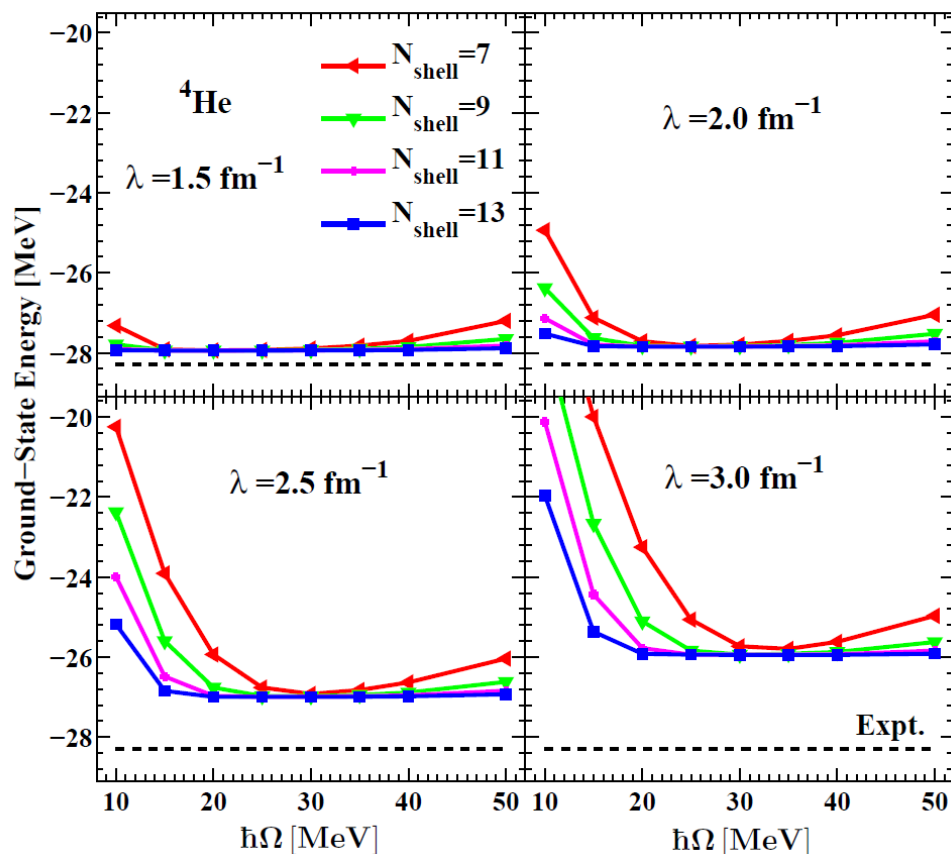
Fig. 3. Ground-state energy of ^4He as a function of $\hbar\Omega$ at four different value (∞ , 3, 2, 1.5 fm^{-1}). The initial potential is the 500 MeV N^3LO NN-only pot from Ref. [13]. The legend from Fig. 1 applies here.

^4He

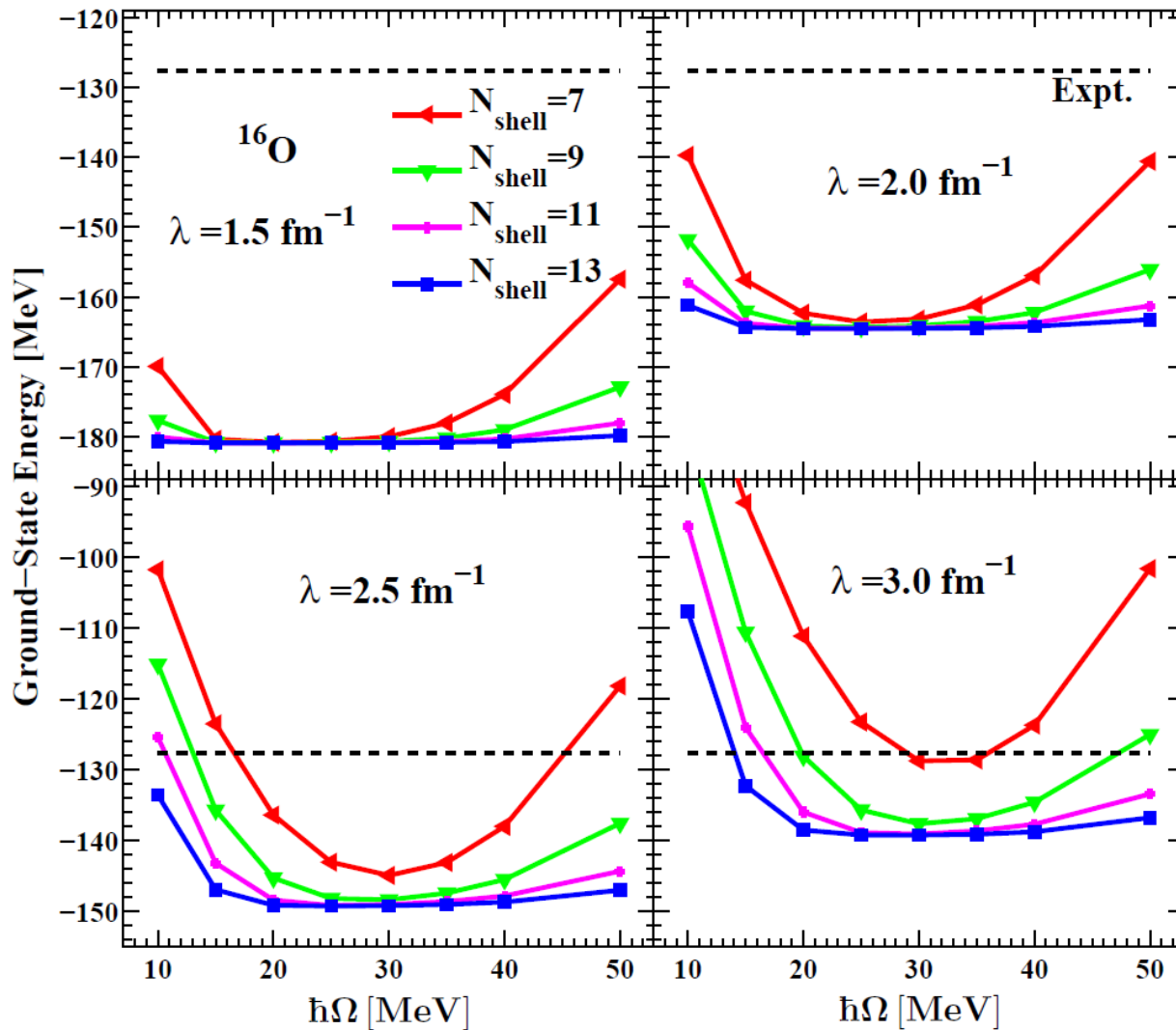
Our MBPT calculations

B.S. Hu, F.R. Xu, Z.H. Sun, J.P. Vary, T. Li,
PRC 94, 014303 (2016)

$\text{N}^3\text{LO} + \text{SRG}$ without 3NF

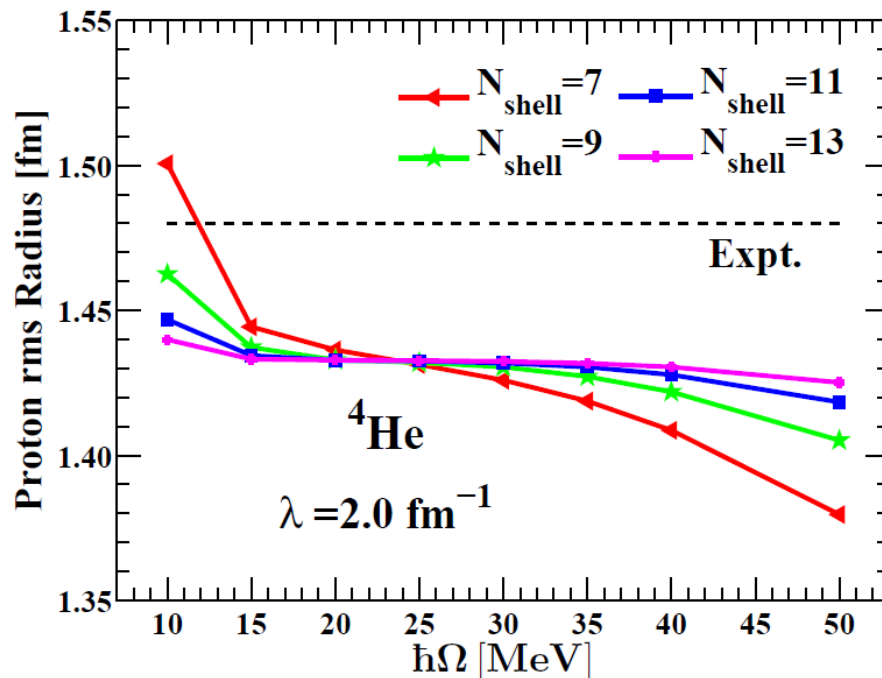
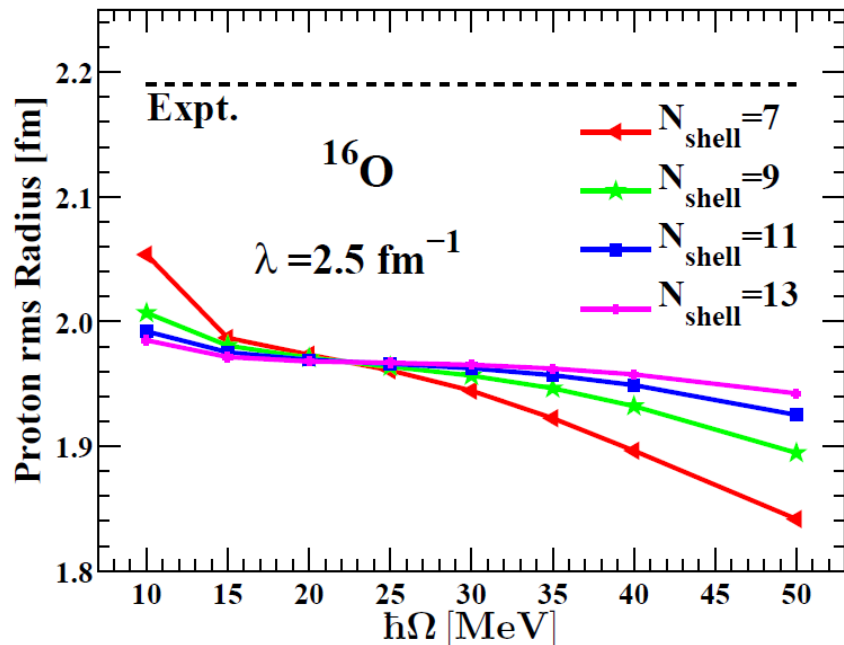


Our MBPT: $N^3\text{LO}+\text{SRG}$ without 3NF



^{16}O

Our MBPT calculations with N³LO+SRG: convergence in radius



R. Roth *et al.* (2006) PRC 73, 044312

AV18, UCOM, corrections to 3rd order in energy, 2nd order in radius

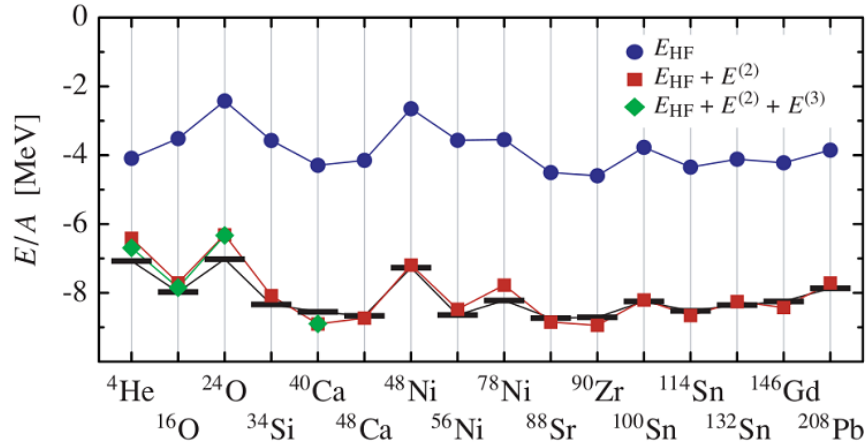


FIG. 5. (Color online) Ground-state energies for selected closed-shell nuclei in HF approximation and with added second- and third-order MBPT corrections. The correlated AV18 potential with $I_\vartheta = 0.09 \text{ fm}^3$ was used. The bars indicate the experimental binding energies [31].

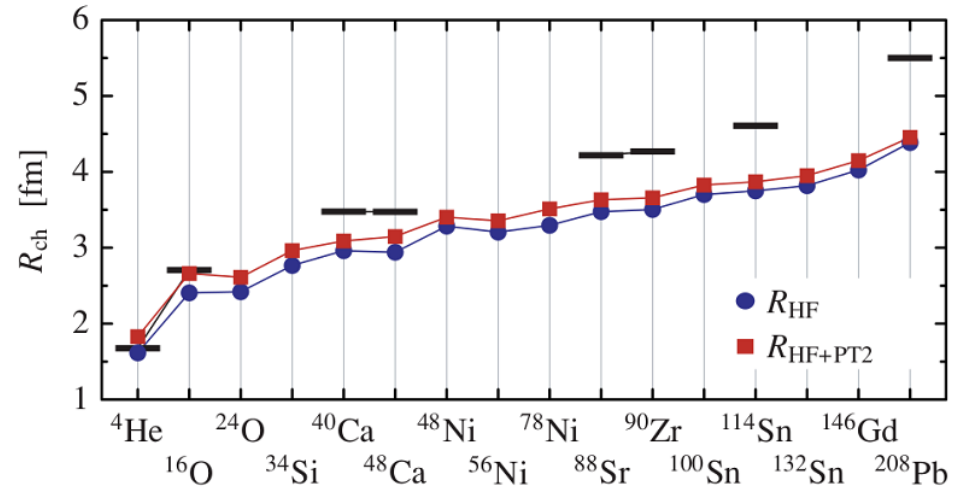


FIG. 8. (Color online) Charge radii for selected closed-shell nuclei in the HF approximation and with added second-order MBPT corrections. The correlated AV18 potential with $I_\vartheta = 0.09 \text{ fm}^3$ was used. The bars indicate experimental charge radii [32].

HF-MBPT calculations for ${}^4\text{He}$ with $\text{N}^3\text{LO-SRG}$, $\text{N}_{\text{shell}}=13$, $\hbar\Omega=35$ MeV

		SRG flow parameter λ (fm $^{-1}$)			
		1.5	2.0	2.5	3.0
Binding energy	Expt. [60]	-28.296	-28.296	-28.296	-28.296
	NCSM [61]	-28.20	-28.41	-27.43	-26.80
	SHF	-25.754	-21.864	-15.854	-10.278
	PT2	-1.788	-5.088	-9.652	-13.783
	PT3	-0.391	-0.899	-1.523	-1.953
	SHF+PT2+PT3	-27.933	-27.850	-27.029	-26.013
		SRG flow parameter λ (fm $^{-1}$)			
		1.5	2.0	2.5	3.0
$r_p(\text{NCSM})=1.418$ fm with $\text{N}_{\text{max}}=10$		1.477	1.477	1.477	1.477
Point-proton rms radius	SHF	1.677	1.652	1.714	1.816
	PT2	0.007	0.001	-0.021	-0.065
	$\Delta r_{\text{c.m.}}$	-0.226	-0.222	-0.227	-0.235
	SHF+PT2+ $\Delta r_{\text{c.m.}}$	1.458	1.431	1.466	1.516

HF-MBPT calculations for ^{16}O with N³LO-SRG, N_{shell}=13, $\hbar\Omega$ =35 MeV

		SRG flow parameter λ (fm ⁻¹)			
		1.5	2.0	2.5	3.0
Binding energy	Expt. [60]	-127.619	-127.619	-127.619	-127.619
	SHF	-169.968	-133.169	-85.173	-44.102
	PT2	-10.132	-29.497	-59.617	-88.326
	PT3	-0.794	-1.931	-4.630	-7.339
	SHF+PT2+PT3	-180.893	-164.597	-149.419	-139.767

3NF important!

		SRG flow parameter λ (fm ⁻¹)			
		1.5	2.0	2.5	3.0
Point-proton rms radius	Expt.	2.581	2.581	2.581	2.581
	SHF	2.098	2.096	2.201	2.345
	PT2	0.011	0.011	-0.006	-0.042
	$\Delta r_{\text{c.m.}}$	-0.067	-0.067	-0.070	-0.073
	SHF+PT2+ $\Delta r_{\text{c.m.}}$	2.042	2.040	2.125	2.230

LQCD → MBPT calculations

LQCD was provided by Aoki and Inoue

We renormalize it using $V_{\text{low-k}}$

Preliminary

$E^{\text{expt}} = -28.3 \text{ MeV}$

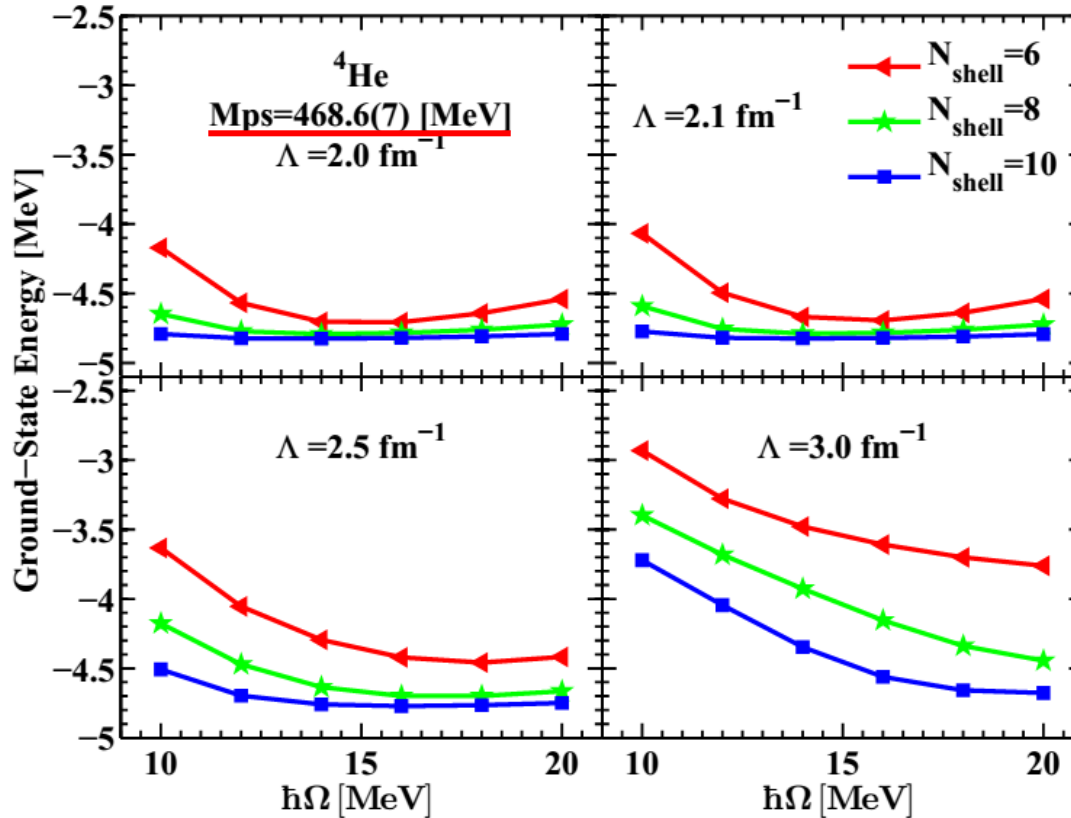


FIG. 6. Ground-state energy of ${}^4\text{He}$ in MBPT calculation as a function of oscillator parameter $\hbar\Omega$ for different $V_{\text{low-k}}$ interactions with $\Lambda = 2.0, 2.1, 2.5, 3.0 \text{ fm}^{-1}$. The initial interaction is the lattice QCD simulations [1–4].

Preliminary

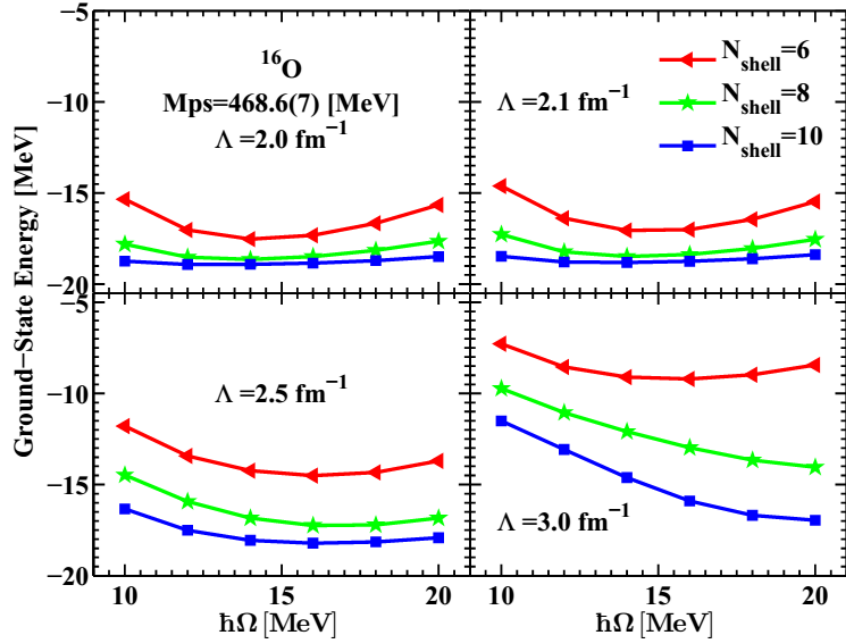


FIG. 7. Ground-state energy of ^{16}O in MBPT calculation as a function of oscillator parameter $\hbar\Omega$ for different $V_{\text{low}k}$ interactions with $\Lambda = 2.0, 2.1, 2.5, 3.0 \text{ fm}^{-1}$. The initial interaction is the lattice QCD simulations [1-4].

$$E^{\text{expt}} = -127.6 \text{ MeV}$$

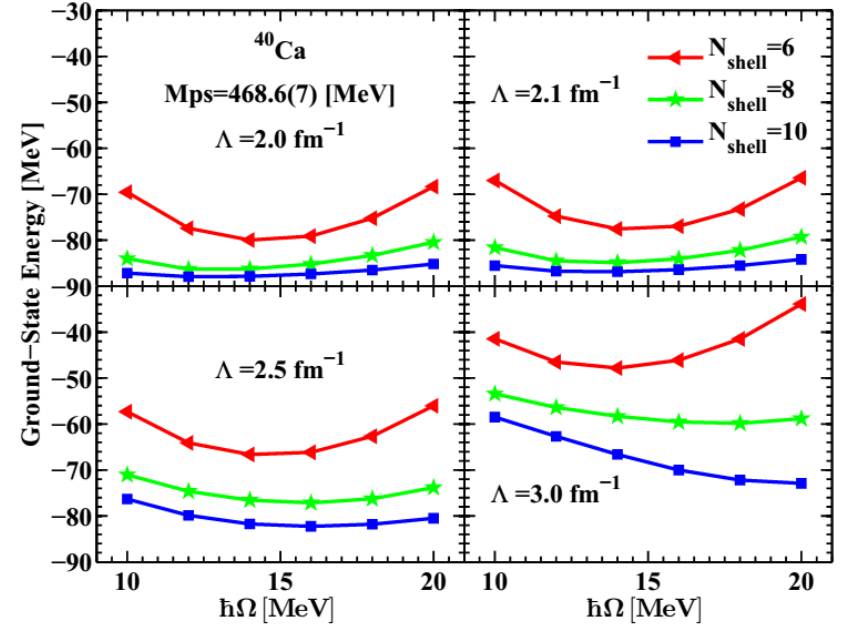
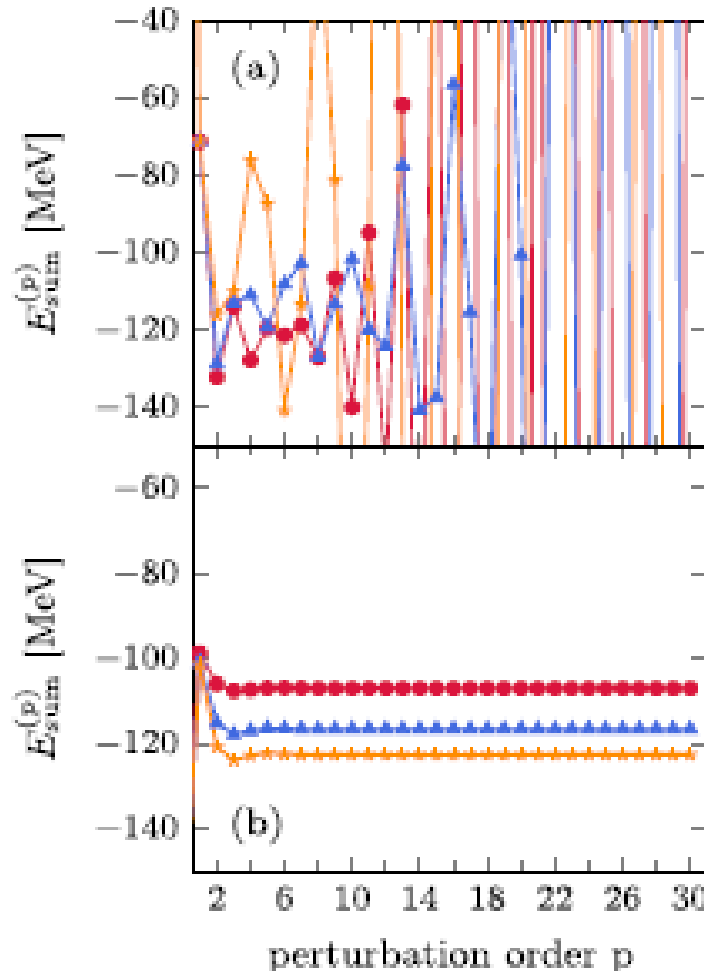


FIG. 8. Ground-state energy of ^{40}Ca in MBPT calculation as a function of oscillator parameter $\hbar\Omega$ for different $V_{\text{low}k}$ interactions with $\Lambda = 2.0, 2.1, 2.5, 3.0 \text{ fm}^{-1}$. The initial interaction is the lattice QCD simulations [1-4].

$$E^{\text{expt}} = -342.0 \text{ MeV}$$

A. Tichaia, J. Langhammera, S. Binder R. Roth, PLB 756 (2016) 283.



MBPT using HO basis

MBPT using HF basis

Fig. 1. Partial sums for the ground-state energy of ^{16}O in the HO basis (a) and the HF basis (b) for the NN+3N-full interaction with $\alpha = 0.08 \text{ fm}^4$ and model-space truncation parameters $N_{\text{max}} = 2$ (\bullet), 4 (\blacktriangle), and 6 (\star). The corresponding energy corrections for each order are displayed in panels (c) and (d), respectively. All calculations are performed at frequency $\hbar\Omega = 24 \text{ MeV}$.

3.2 HF-RPA calculations for multipole giant resonances

- i) Chiral EFT potential NNLO_{sat} (NN + NNN)
- ii) Hartree-Fock + Random Phase Approximation (RPA)
- iii) Multipole giant resonances (monopole, dipole and quadrupole)

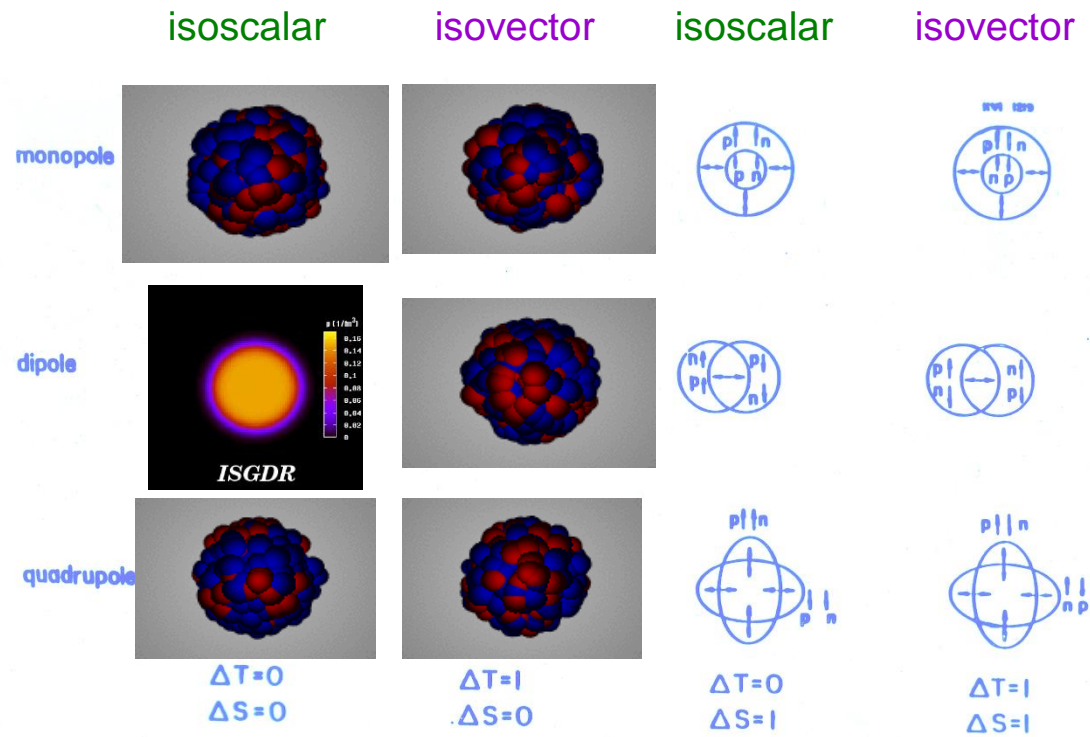
$$H = \sum_{i=1}^A \frac{\mathbf{p}_i^2}{2m} + \sum_{i<j=1}^A V_{ij} - \frac{(\sum_{i=1}^A \mathbf{p}_i)^2}{2mA} + \sum_{i<j<k=1}^A W_{ijk}$$

Performing spherical HF

$$= (1 - \frac{1}{A}) \sum_{i=1}^A \frac{\mathbf{p}_i^2}{2m} + \sum_{i<j=1}^A (V_{ij} - \frac{\mathbf{p}_i \cdot \mathbf{p}_j}{mA}) + \sum_{i<j<k=1}^A W_{ijk}$$

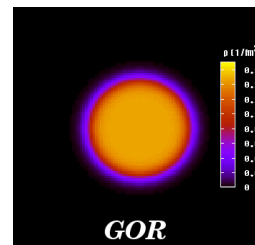
$$W_{\text{NO}} = \frac{1}{6} \sum_{ijk} \langle ijk | W | ijk \rangle + \frac{1}{2} \sum_{ijps} \langle pij | W | sij \rangle \{a_p^\dagger a_s\} + \frac{1}{4} \sum_{ipqst} \langle pqi | W | sti \rangle \{a_p^\dagger a_q^\dagger a_t a_s\} +$$
$$\frac{1}{36} \sum_{pqrst} \langle pqr | W | stu \rangle \{a_p^\dagger a_q^\dagger a_r^\dagger a_u a_t a_s\}, \quad \text{NNN normal ordering for RPA calculation}$$

Nuclear giant resonances



Electric

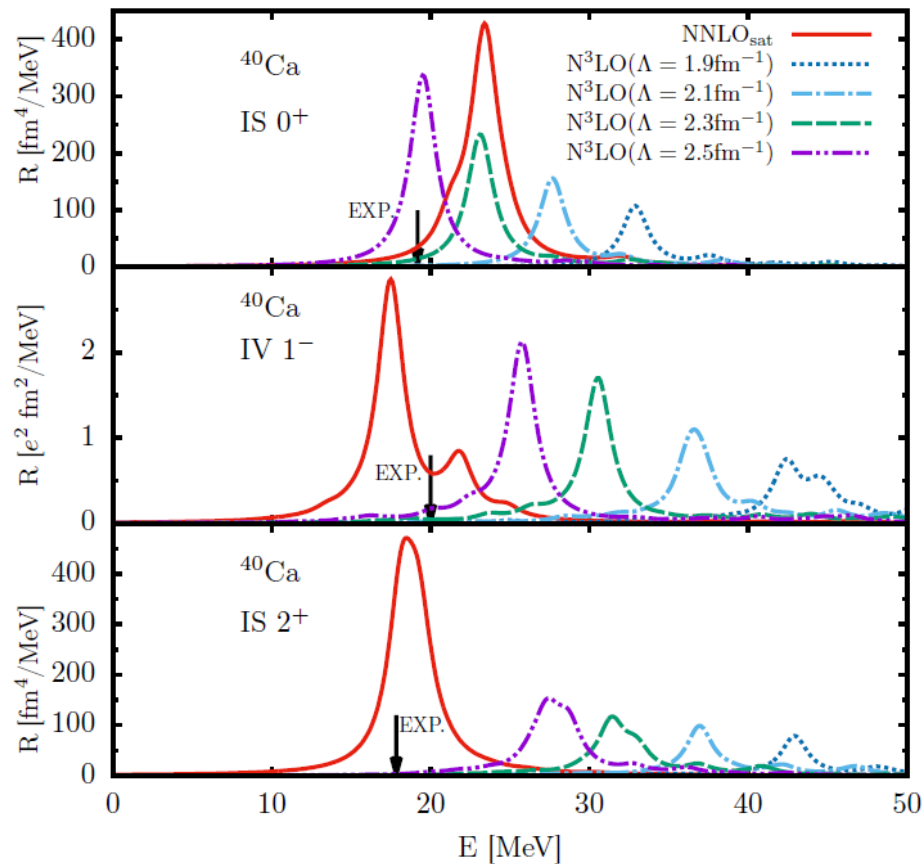
Magnetic



animations courtesy M. Itoh and T. Aumann

From U. Garg

HF-RPA calculations with $N^3\text{LO}$ (NN) and NNLO_{sat} (NN+NNN)

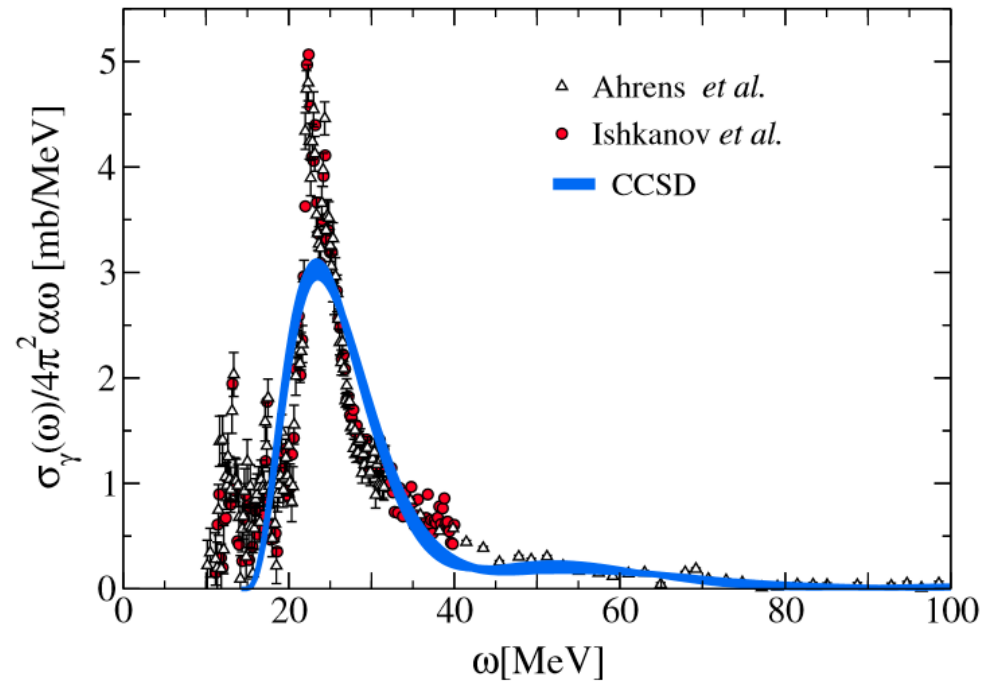
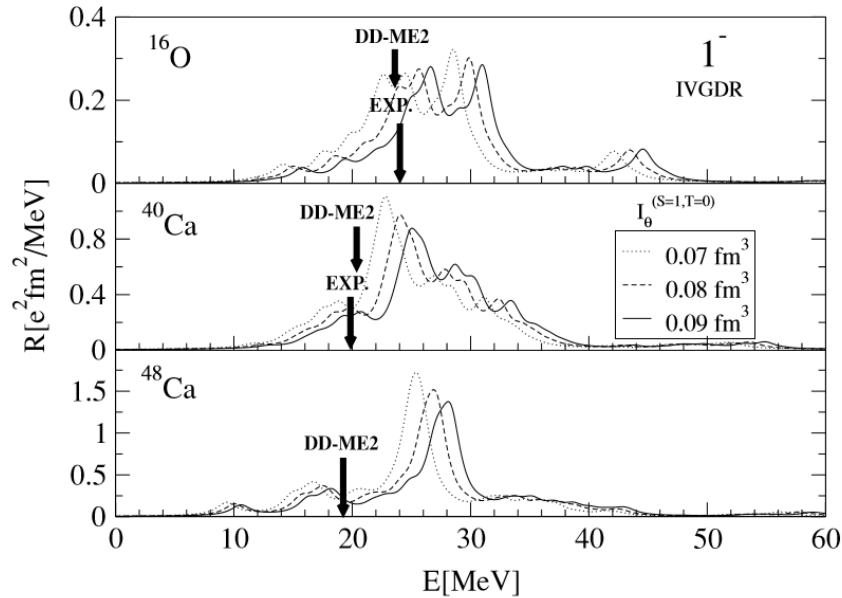


$N^3\text{LO}$ (NN) without NNN calculations are sensitive to the momentum cutoff Λ in $V_{\text{low-k}}$.

One cannot find a single Λ value to describe simultaneously the different types of resonances.

AV18 UCOM RPA

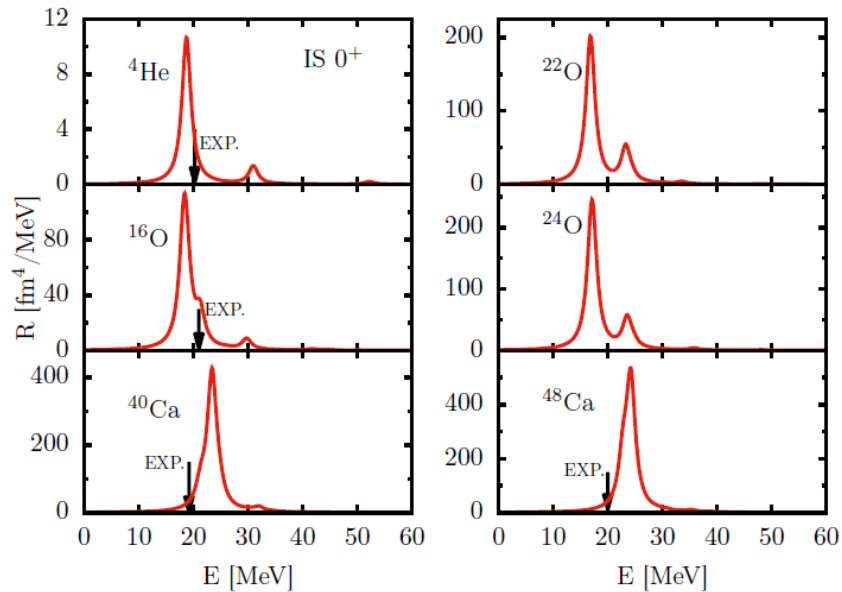
N. Paar, P. Papakonstantinou, H. Hergert, R. Roth, PRC 74, 014318 (2006)



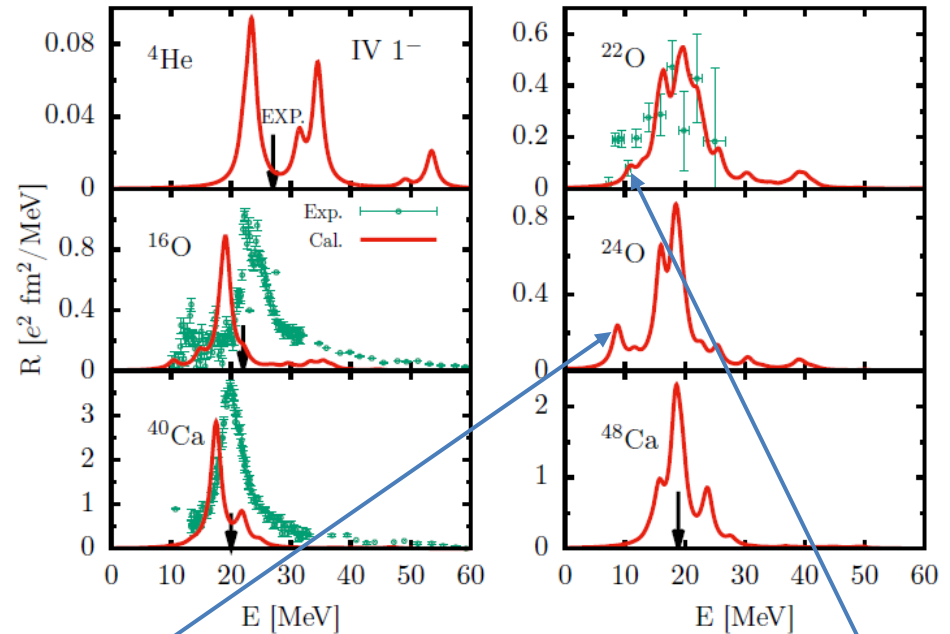
^{16}O , IVGDR, CCSD with bare N3LO(NN)
S. Bacca, N. Barnea, G. Hagen, G. Orlandini,
T. Papenbrock, PRL 111, 122502 (2013)

NNLO_{sat} HF-RPA

ISGMR



IVGDR

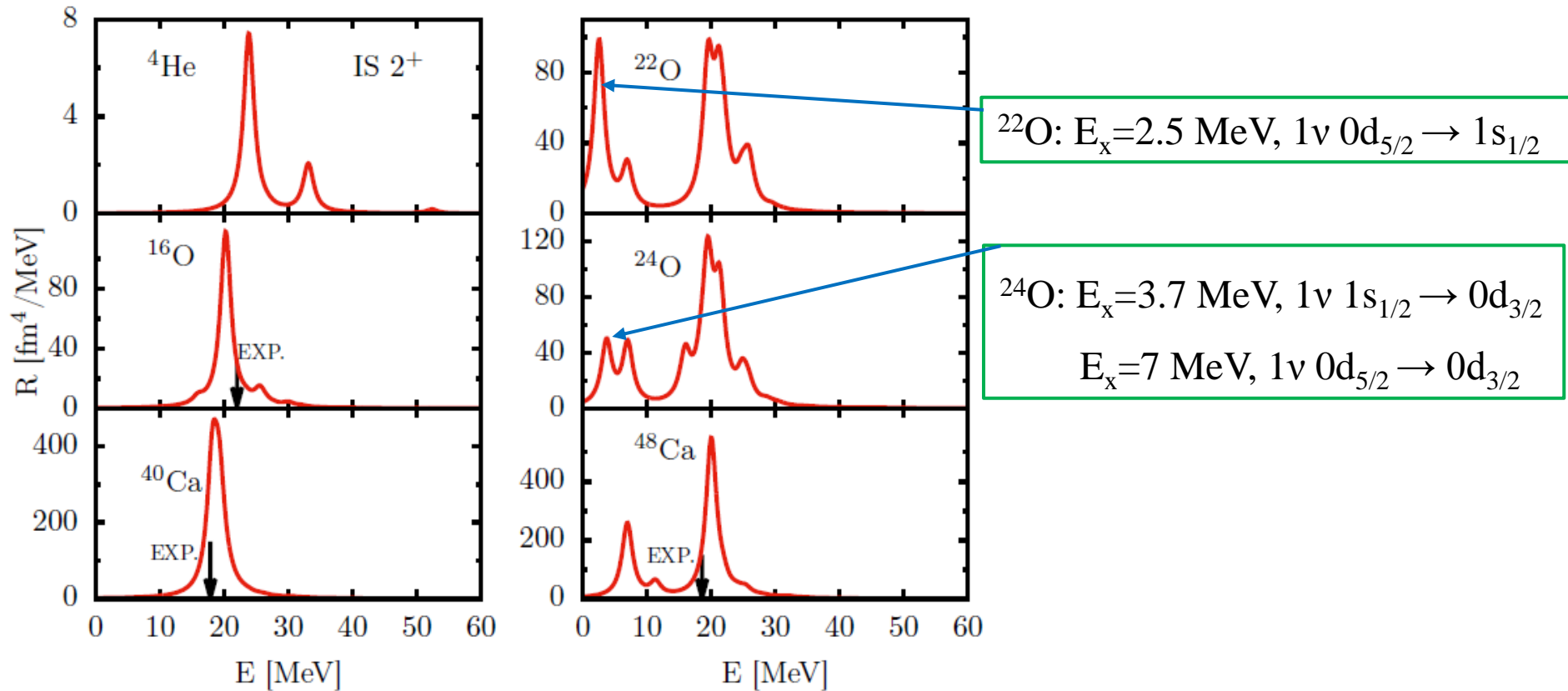


^{24}O : 8.7 MeV
 Neutron
 excitations:

87% $1s_{1/2} \rightarrow 1p_{3/2}$
 5% $0d_{5/2} \rightarrow 0f_{7/2}$

^{22}O : 10.8 MeV
 Neutron
 excitations:

62% $0d_{5/2} \rightarrow 1p_{3/2}$
 15% $0p_{1/2} \rightarrow 1s_{1/2}$
 8% $0d_{5/2} \rightarrow 0f_{7/2}$



GSM

$^{22}\text{O}: E(2_1^+)=3.3 \text{ MeV}, 1\nu 0d_{5/2} \rightarrow 1s_{1/2}$

$^{24}\text{O}: E(2_1^+)=4.5 \text{ MeV}, 1\nu 1s_{1/2} \rightarrow 0d_{3/2}$

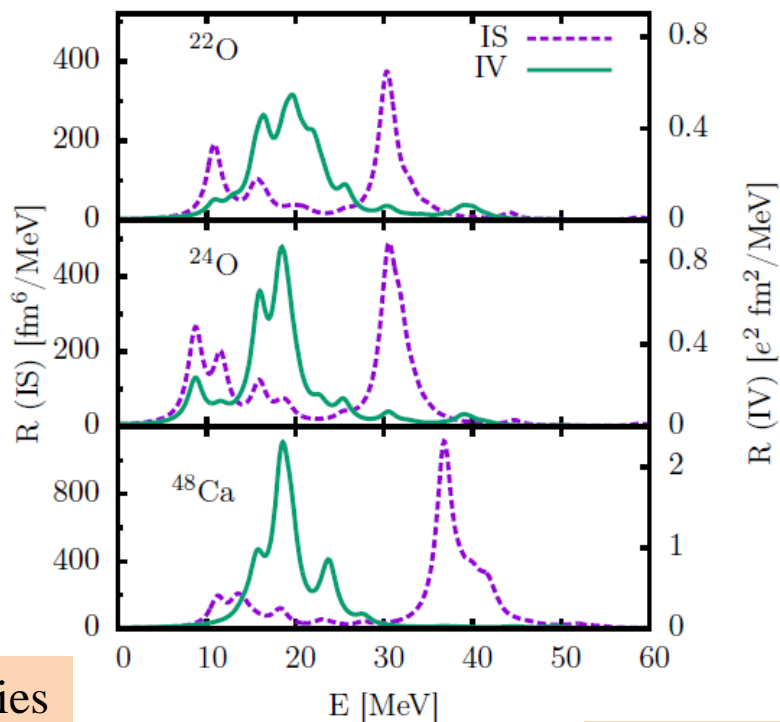
Expt

$^{22}\text{O}: E(2_1^+)=3.2 \text{ MeV}$

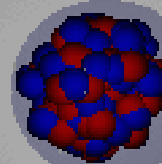
$^{24}\text{O}: E(2_1^+)=4.7 \text{ MeV}$

NNLO_{sat} HF-RPA

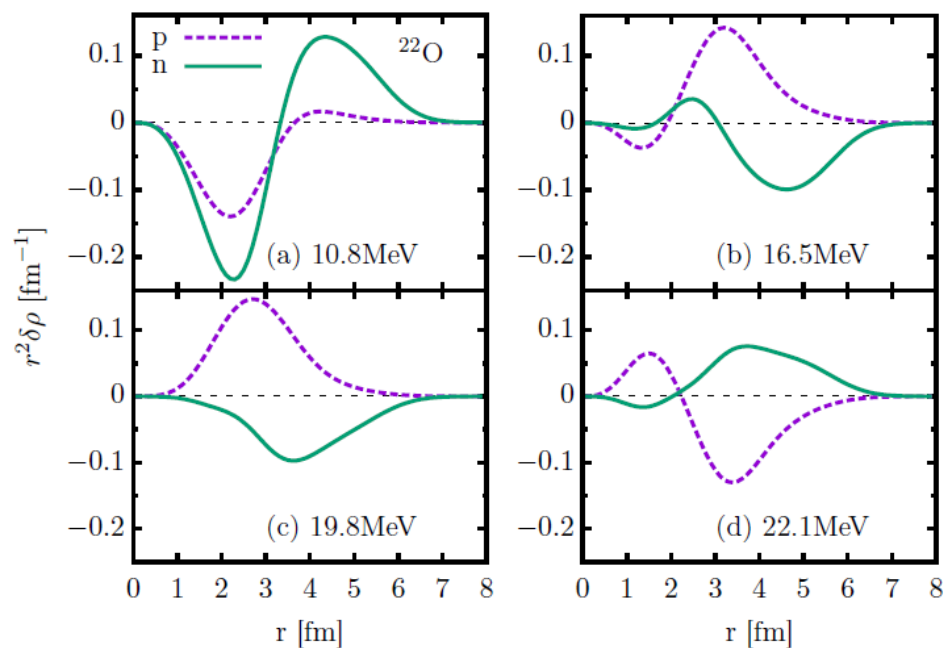
Dipole resonances



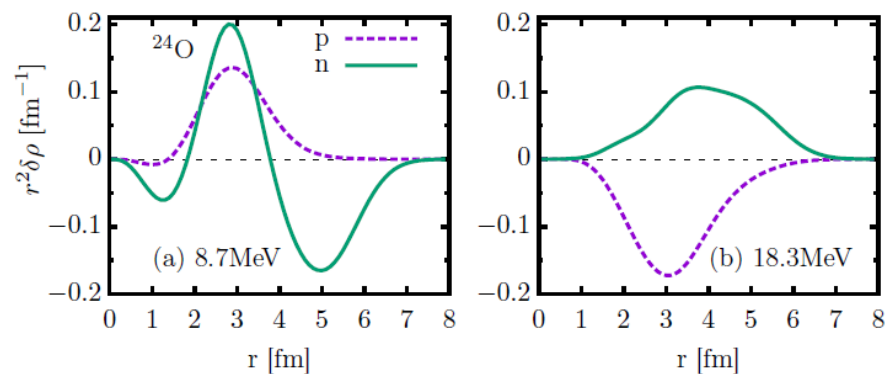
Pygmy Resonance



Transition densities



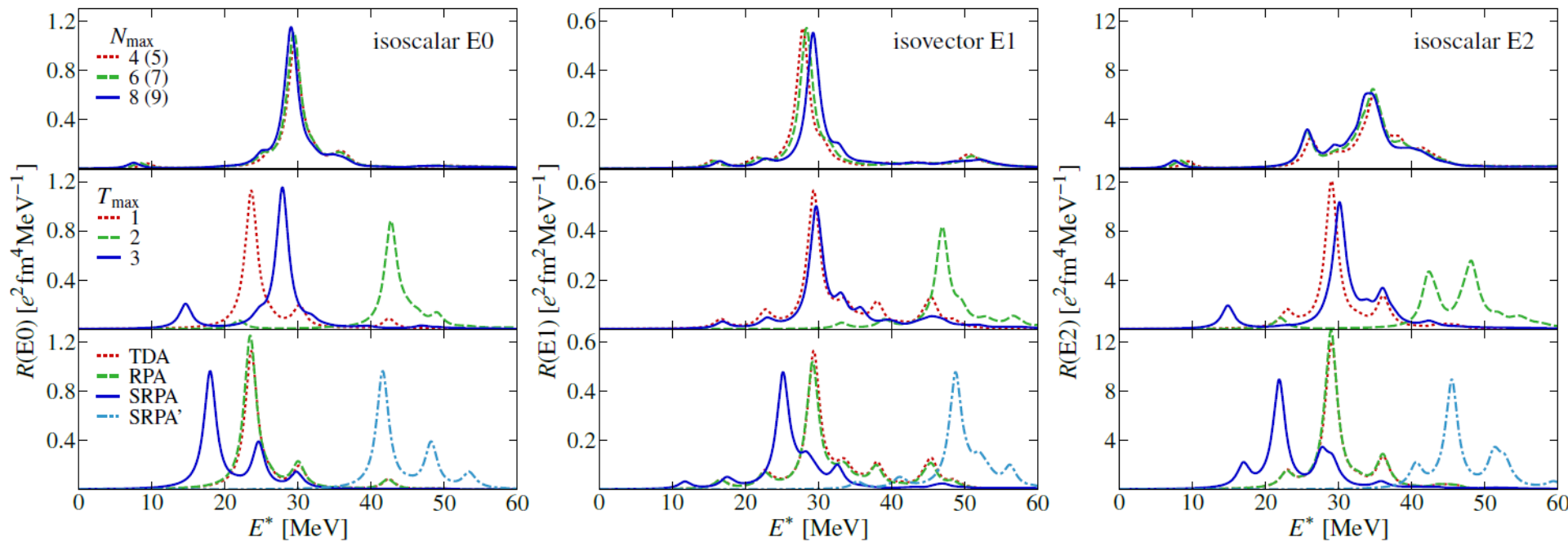
Transition densities



$$\delta \rho_{\nu}^J(r) = \sum_{\mu} \langle \nu | \sum_i \frac{\delta(r - r_i)}{r^2} Y_{J\mu}(\hat{r}_i) | 0 \rangle$$

3NFs (high-order forces) may be important for descriptions of nuclear giant resonances.

How about high-order many-body correlations? RPA considers only 1p1h correlation.

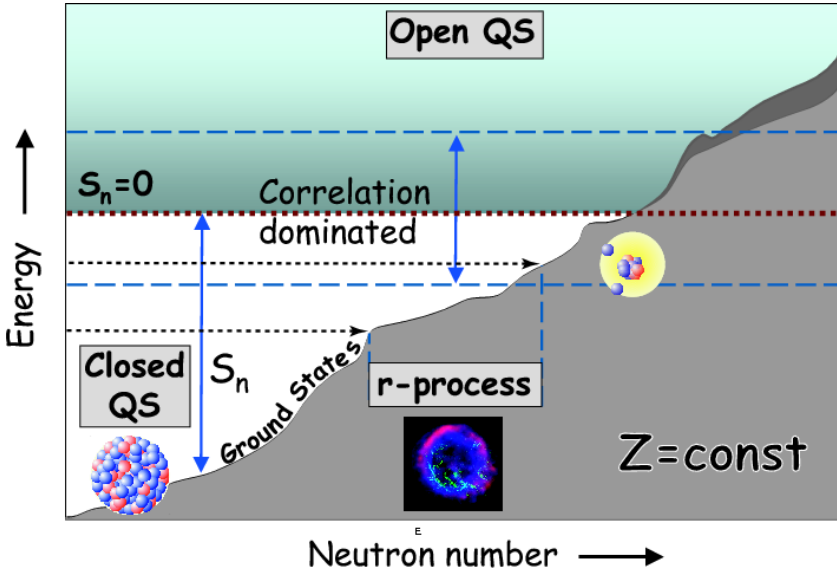


^{16}O , SRG $\text{N}^3\text{LO}(\text{NN}) + \text{N}^2\text{LO}(\text{NNN})$ NCSM in HF basis

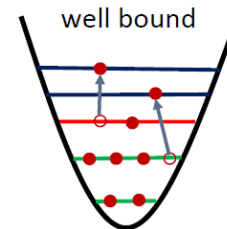
C. Stumpf, T. Wolfgruber, R. Roth, arXiv:1709.06840v1 [nucl-th] 20 Sep 2017

RPA 1p1h approach seems good!

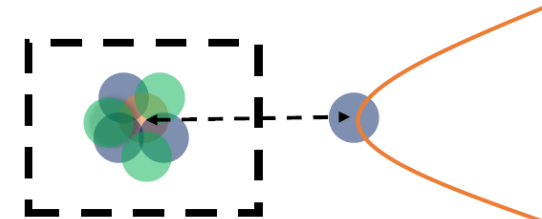
3.3 Gamow Shell Model (GSM) for resonance and continuum in weakly bound nuclei



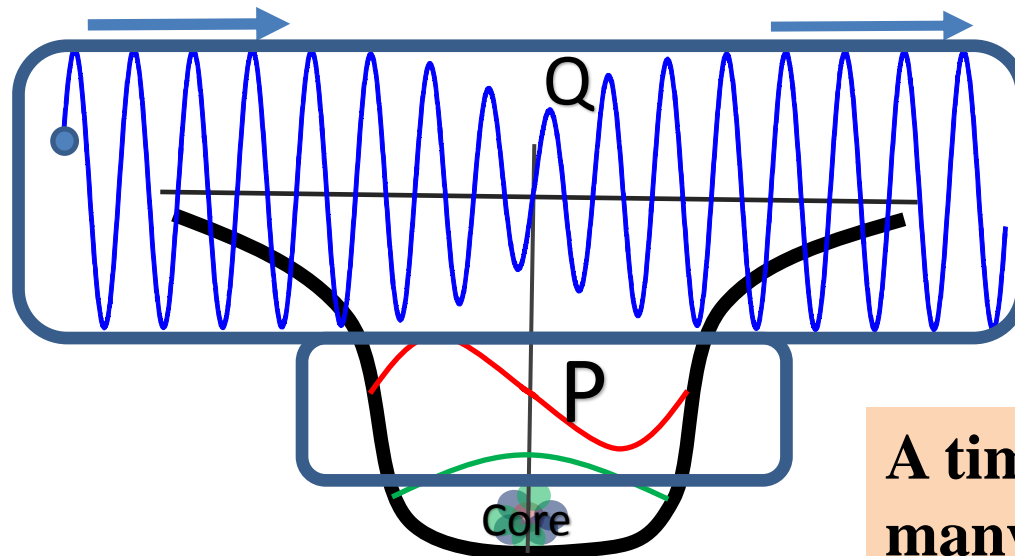
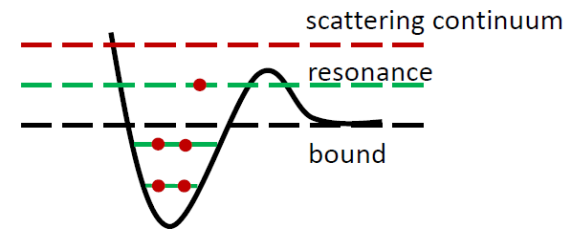
Closed quantum system



HO basis



Open quantum system



A time-dependent many-body problem

Gamow Shell Model

T. Berggren, Nucl. Phys. A109 (1968) 265

Single-particle basis in complex- k plane describe bound, resonance and scattering on equal footing.

The radial wave function $u(r)/r$

$$\frac{d^2 u(k, r)}{dr^2} = \left[\frac{l(l+1)}{r^2} + \frac{2m}{\hbar^2} U(r) - k^2 \right] u(k, r)$$

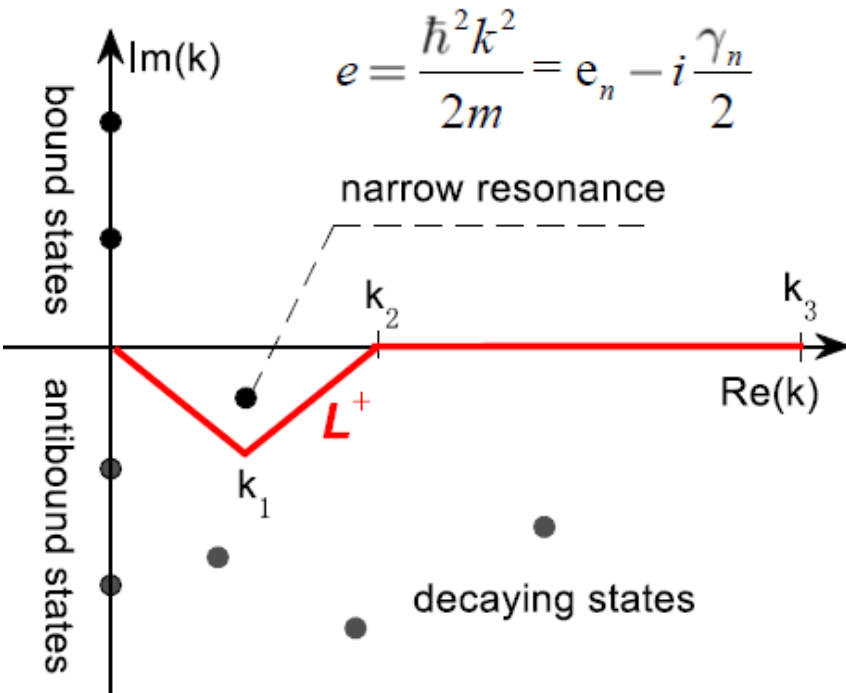
boundary conditions

$$u(0) = 0,$$

$$u(a)O_l'(ka) - u'(a)O_l(ka) = 0$$

$$O_l(kr) \sim e^{i(kr - l\pi/2)}$$

Outgoing solution at large distance



Orthogonality and Completeness

$$\delta(r - r') = \sum_n w_n(r, k_n) w_n(r', k_n) + \frac{1}{\pi} \int_{L^+} dq u(r, q) u(r', q)$$

Discretized

Woods-Saxon potential, CD-Bonn, ^{16}O core

$0d_{3/2}$ ████████ 1.06-0.089i

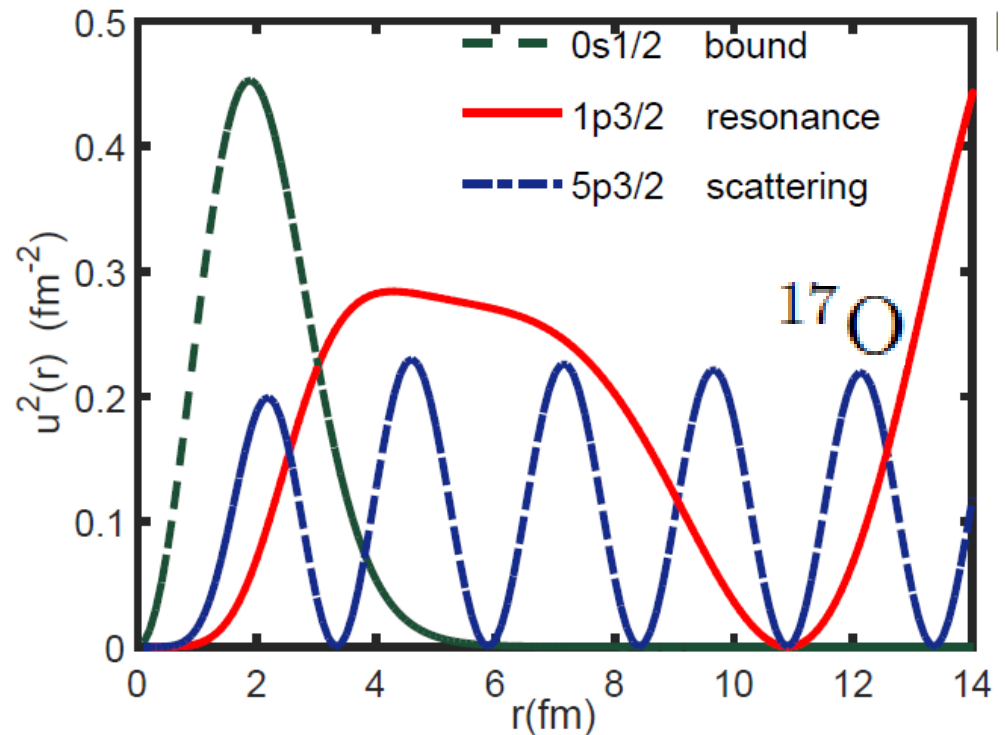
----- $e=0.0$

$1s_{1/2}$ ████████ -3.22-0.00i

$0d_{5/2}$ ████████ -5.31-0.00i (MeV)

WS SPE's

$$e = \frac{\hbar^2 k^2}{2m} = e_n - i \frac{\gamma_n}{2}$$



CGSM based on realistic nuclear forces

Realistic nuclear forces \rightarrow Gamow shell model calculations

Taking a doubly closed core

Bare forces:
Strong repulsion,
slow convergence

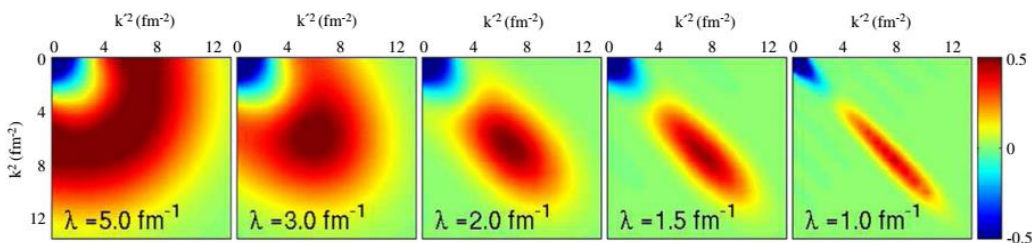
$V_{low k}$ or SRG

To remove hard core,
but still keep good
descriptions of NN
scattering phase shifts

$$\langle \alpha_P | \bar{H}_{\text{eff}} | \alpha_{P'} \rangle = \sum_{\alpha_{P''}} \sum_{\alpha_{P'''}} \sum_{kk'k'' \in \mathcal{K}} \langle \alpha_P | \tilde{k}'' \rangle \langle \tilde{k}'' | \alpha_{P''} \rangle \langle \alpha_{P''} | \tilde{k} \rangle E_k \langle \tilde{k} | \alpha_{P'''} \rangle \langle \alpha_{P'''} | \tilde{k}' \rangle \langle \tilde{k}' | \alpha_{P'} \rangle$$

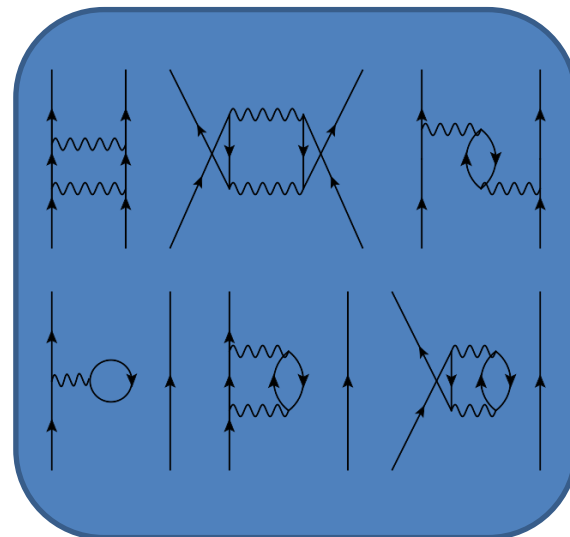
$$\frac{dH_\lambda}{d\lambda} = -\frac{4}{\lambda^5} [[T_{\text{rel}}, H_\lambda], H_\lambda]$$

Q



$$H_{\text{eff}} = \hat{Q} - \hat{Q} \int \hat{Q} + \hat{Q} \int \hat{Q} \int \hat{Q} - \dots$$

$$\hat{Q}(E) = PVP + PVQ \frac{1}{E - H} QVP,$$



Non-degenerate extended Kuo-Krenciglowa folded-diagram method (EKK) by Takayanagi, NPA 852, 61 (2011);

Continuum

⋮

$g_{9/2} \dots$

$1p_{1/2}, 2p_{1/2} \dots$

$f_{5/2} \dots$

$1p_{3/2}, 2p_{3/2} \dots$

$f_{7/2} \dots$

$d_{3/2}$ channel

$1d_{3/2}, 2d_{3/2} \dots$

Model space

$0d_{3/2}$

$0d_{3/2}$

$1s_{1/2}$

$1s_{1/2}$

$0d_{5/2}$

$0d_{5/2}$

$0p_{1/2}$

$0p_{3/2}$

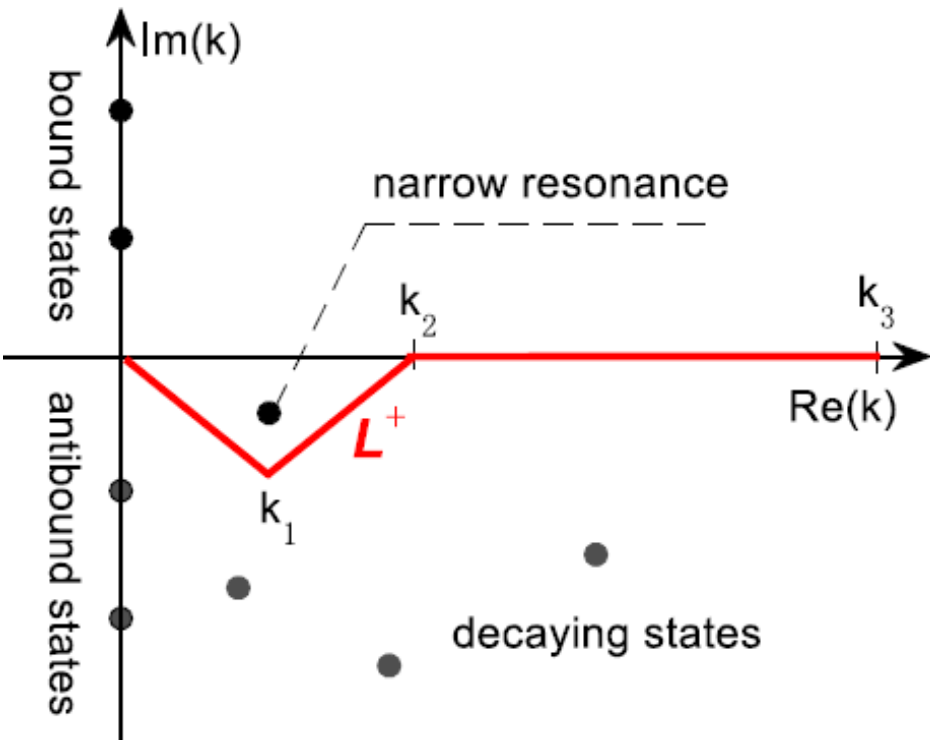
$0s_{1/2}$

8

2

Q-box folded diagrams in **complex-k** basis

Convergence against
discretization number N_L



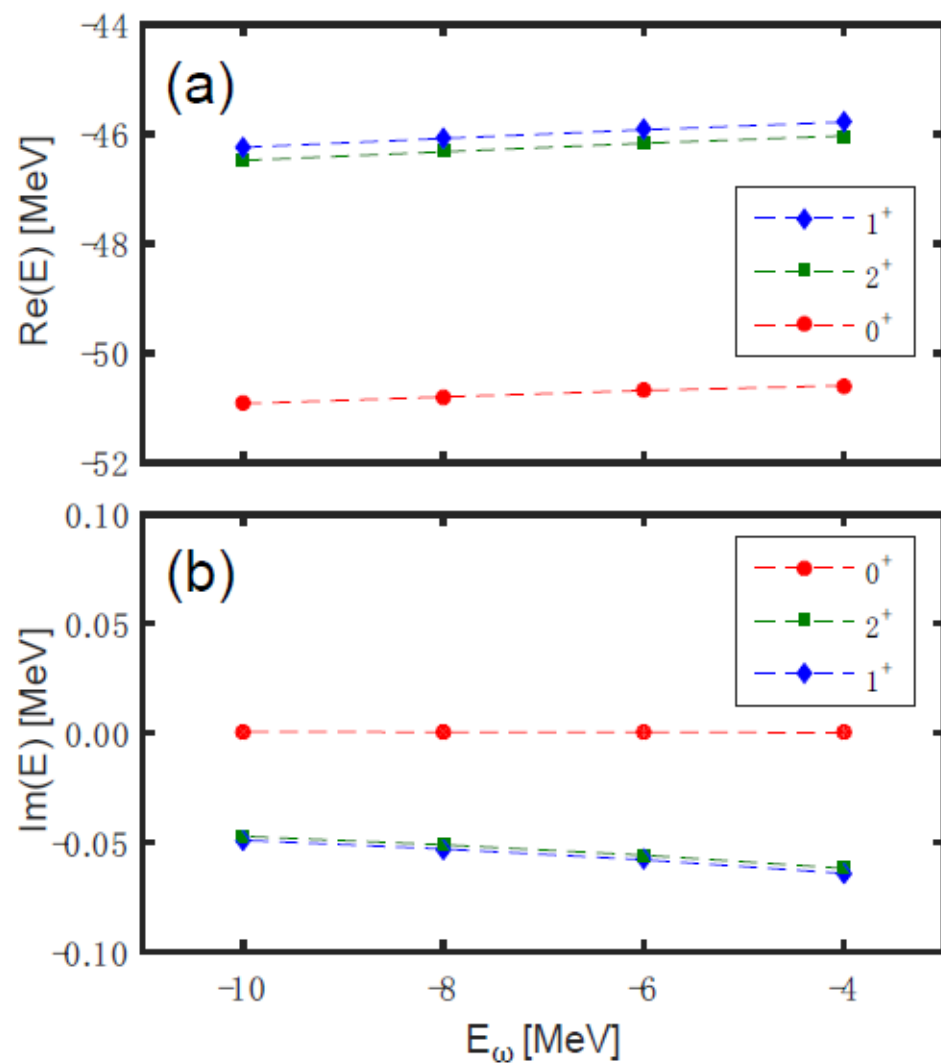
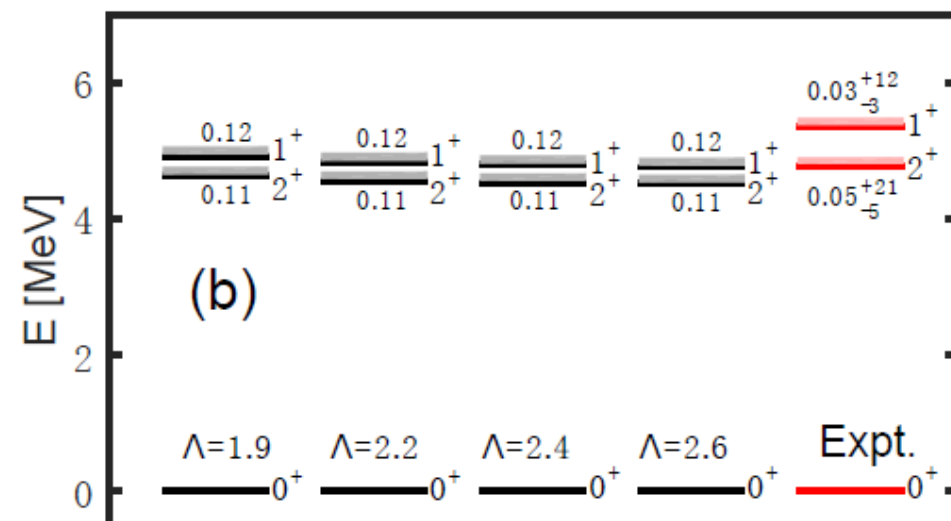
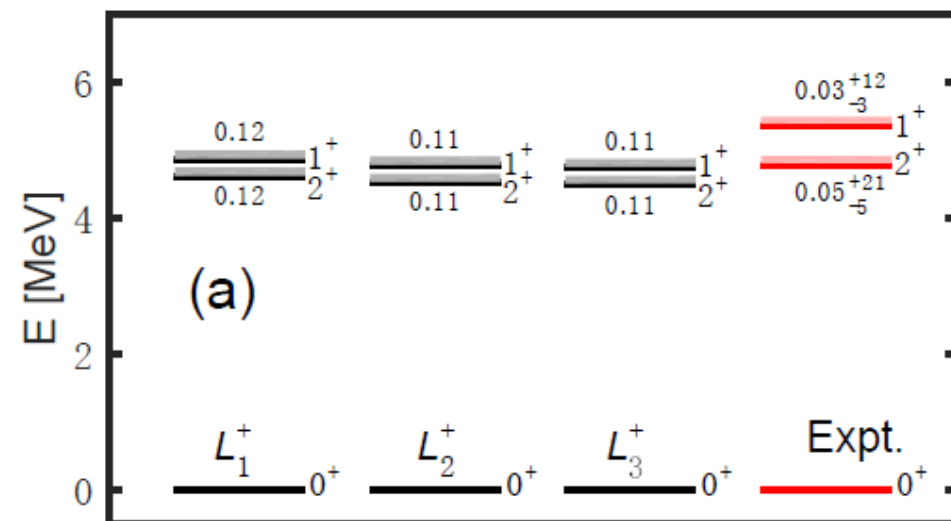
$$\tilde{E}_n = E_n - i\Gamma/2$$

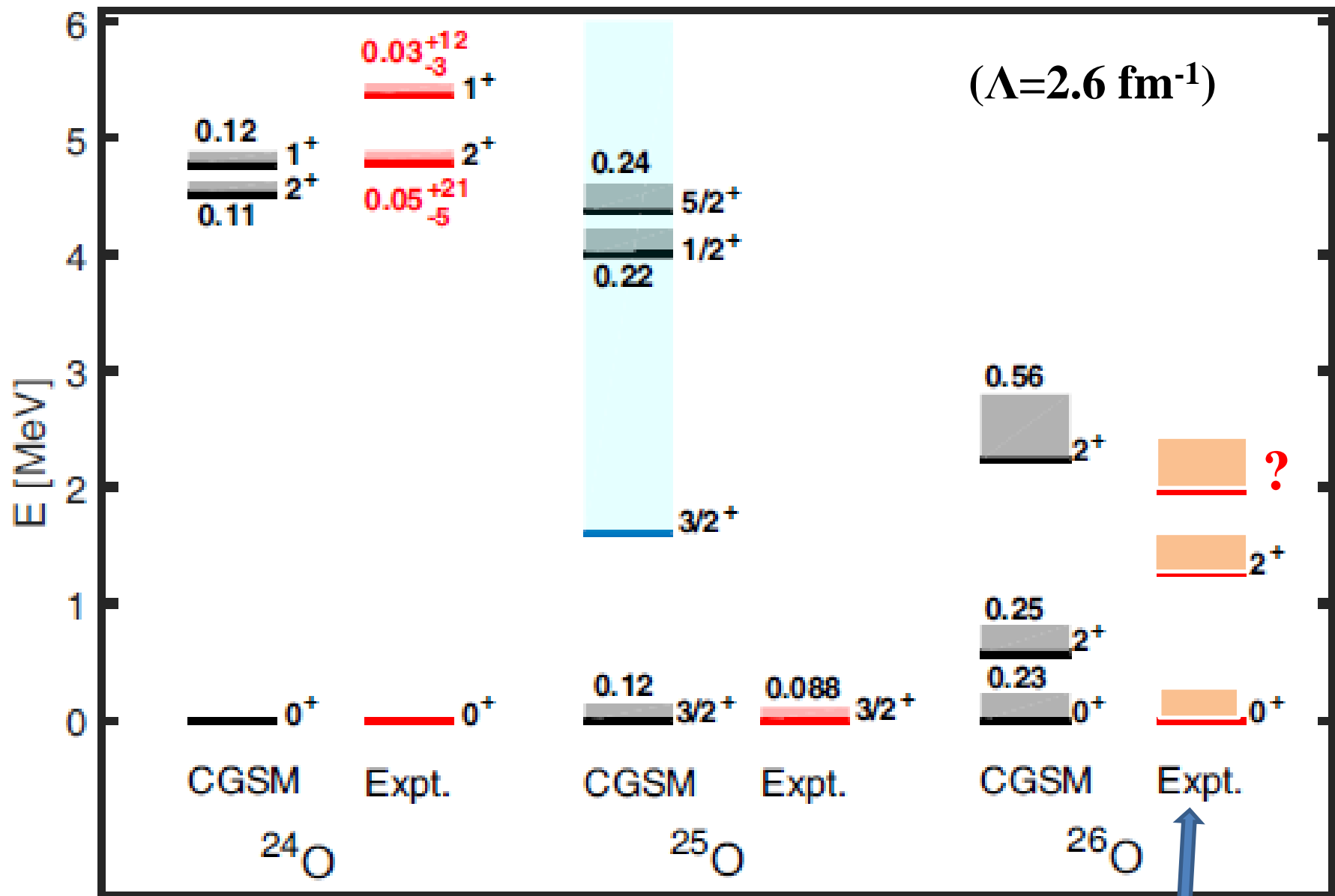
^{24}O
 $\Lambda = 2.6 \text{ fm}^{-1}$

N_L	0^+	2^+	1^+
16	$-50.642 + 0.013i$	$-46.172 - 0.004i$	$-45.922 - 0.009i$
18	$-50.716 + 0.002i$	$-46.262 - 0.046i$	$-46.017 - 0.049i$
20	$-50.711 - 0.001i$	$-46.219 - 0.054i$	$-45.976 - 0.056i$
22	$-50.712 + 0.000i$	$-46.218 - 0.053i$	$-45.974 - 0.056i$

Convergences of spectroscopic calculations

^{24}O





Y. Kondo *et al.*, PRL 116, 102503 (2016)

Binding energies, one-neutron separation energies

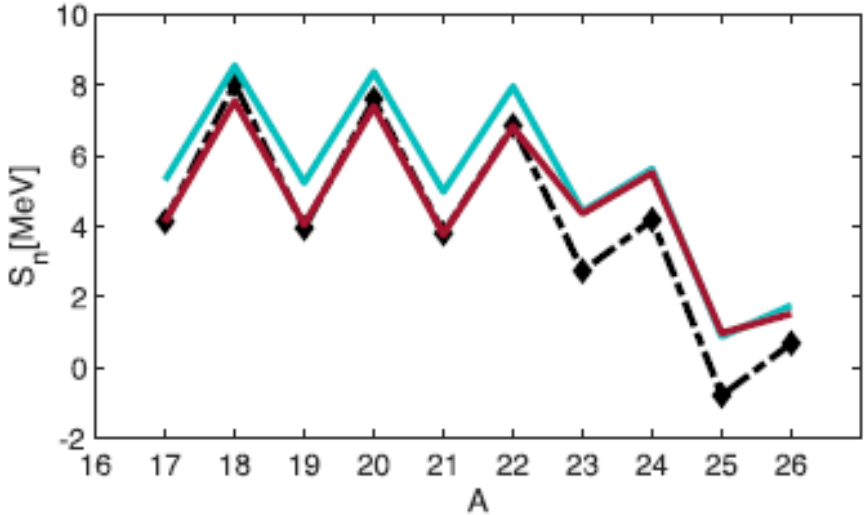
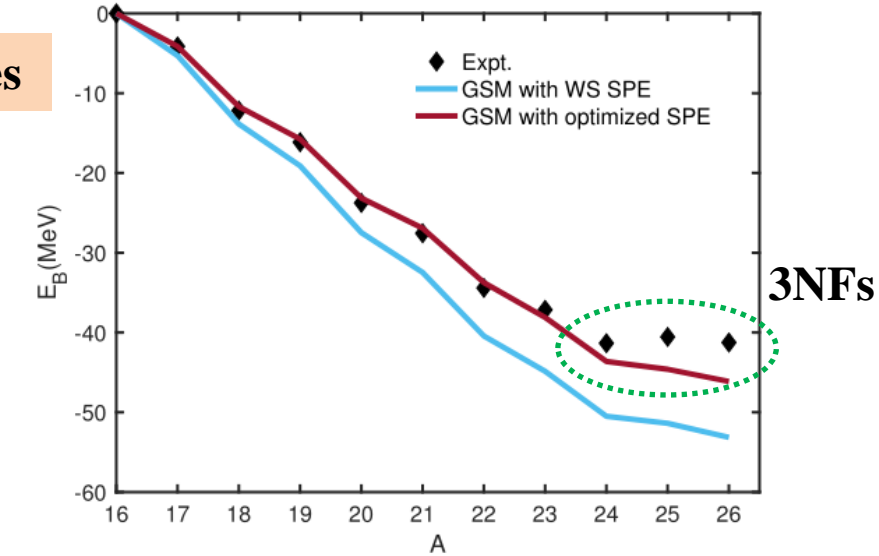
$$\tilde{e}_n = e_n - i\gamma_n/2$$

$0d_{3/2}$ ██████████ **1.06-0.089i** ██████████ **0.94-0.048i**
----- **e=0.0**

$1s_{1/2}$ ██████████ **-3.22-0.00i** ██████████ **-3.27-0.00i**
██████████ **-4.14-0.00i**

$0d_{5/2}$ ██████████ **-5.31-0.00i (MeV)**

WS SPE's Expt. SPE's
[Extracted from ^{17}O ,
by Michel *et al.*, PRC 67, 054311 (2003)]



Summary

- 1) **$N^3LO(NN)$ + Hartree-Fock + MBPT for closed-shell nuclei**
- 2) **$NNLO_{\text{sat}}(NN+NNN)$ + Hartree-Fock + RPA for nuclear giant resonances**
3. **CD Bonn (NN) + $V_{\text{low-}k}$ + CGSM with resonance and continuum for weakly-bound nuclei**



Thank you for your
attention

F.R. Xu, B. S. Hu, Z.H. Sun, Q. Wu, J. Vary, G. R. Jansen

**Many-body perturbation theories in modern quantum chemistry and nuclear physics,
March 26-30, 2018, CEA, Saclay, France**